ELSEVIER

Contents lists available at ScienceDirect

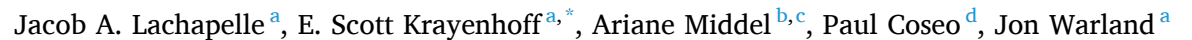
Landscape and Urban Planning

journal homepage: www.elsevier.com/locate/landurbplan



Research Paper

Maximizing the pedestrian radiative cooling benefit per street tree



- ^a School of Environmental Sciences, University of Guelph, Guelph, Ontario, Canada
- ^b School of Arts, Media and Engineering, Arizona State University, Tempe, AZ, USA
- ^c School of Computing and Augmented Intelligence, Arizona State University, Tempe, AZ, USA
- ^d The Design School, Arizona State University, Tempe, AZ, USA

HIGHLIGHTS

- Efficiency of street tree radiative cooling depends on tree placement.
- TUF-Pedestrian model quantifies impact of sidewalk tree spacing on pedestrian TMRT.
- Spatial variation of directional longwave radiation loading on pedestrians captured.
- More sidewalk tree cover increases TMRT reduction with modestly diminishing returns.
- Equally-spaced trees among warm season sun-exposed pedestrian routes optimize cooling.

ARTICLE INFO

Keywords: Pedestrian thermal comfort Urban forestry Microclimate modelling Radiative heat exposure Green infrastructure design Sidewalk shade

ABSTRACT

Outdoor heat stress is a growing problem in cities during hot weather. City planners and designers require more pedestrian-centered approaches to understand sidewalk microclimates. Radiation loading, as quantified by mean radiant temperature (T_{MRT}), is a key factor driving poor thermal comfort. Street trees provide shade and consequently reduce pedestrian T_{MRT}. However, placement of trees to optimize the cooling they provide is not yet well understood. We apply the newly-developed TUF-Pedestrian model to quantify the impacts of sidewalk tree coverage on pedestrian T_{MRT} during summer for a lowrise neighbourhood in a midlatitude city. TUF-Pedestrian captures the detailed spatio-temporal variation of direct shading and directional longwave radiation loading on pedestrians resulting from tree shade. We conduct 190 multi-day simulations to assess a full range of sidewalk street tree coverages for five high heat exposure locations across four street orientations. We identify street directions that exhibit the largest T_{MRT} reductions during the hottest periods of the day as a result of tree planting. Importantly, planting a shade tree on a street where none currently exist provides approximately 1.5-2 times as much radiative cooling to pedestrians as planting the same tree on a street where most of the sidewalk already benefits from tree shade. Thus, a relatively equal distribution of trees among sun-exposed pedestrian routes and sidewalks within a block or neighbourhood avoids mutual shading and therefore optimizes outdoor radiative heat reduction per tree during warm conditions. Ultimately, street tree planting should be a place-based decision and account for additional environmental and socio-political factors.

1. Introduction

Pedestrians in many cities experience excessive daytime heat in the summertime or warm season (Oke et al., 1991; Oke et al., 2017). More worrisome, episodes of excessive heat are expected to increase with more frequent and intense heat waves due to climate change (Dosio, Mentaschi, Fischer, & Wyser, 2018). At the same time, many cities are

encouraging people to walk more to reduce greenhouse gas emissions and reach other sustainability and health objectives. For example, thermally uncomfortable outdoor urban spaces may contribute to making cities obesogenic. In addition, pedestrian spaces, such as sidewalks, are critical infrastructure that support a public commons of informal social contact, helping maintain societal understandings of diverse social structures – knowing about others and their challenges

^{*} Corresponding author at: 50 Stone Road East, Guelph, Ontario N1G 2W1, Canada.

E-mail addresses: jlachape@uoguelph.ca (J.A. Lachapelle), skrayenh@uoguelph.ca (E. Scott Krayenhoff), ariane.middel@asu.edu (A. Middel), paul.coseo@asu.edu (P. Coseo), jwarland@uoguelph.ca (J. Warland).

(Duneier, 2001; Gehl, 1987; Jacobs, 1961). Walkability goals aim to make neighbourhoods more walkable and social through compact development with traversable, enjoyable, and safe pedestrian infrastructure (e.g. sidewalks, street trees, benches) (Forsyth, 2015). Even lower density communities are investing in transitions to more walkable pedestrian infrastructure (McGreevy, Musolino, Udell, & Baum, 2021). Yet, an increasing societal push toward walking combined with increasing heat may make pedestrians more prone to heat stress without sufficient optimization of sidewalk microclimate design (Dzyuban et al., 2022). To improve pedestrian thermal comfort, city officials, planners, and designers require guidance on management of pedestrian overheating that accounts for three-dimensional street design (including shading effects), building wall and pavement materials, and vegetation type and placement.

A key contributor to overheating of pedestrians in cities is the large coverage of impermeable surfaces, which, unlike permeable surfaces, can divert little of their high warm season radiant loads to latent heat, and instead warm the air, the subsurface, and radiate strongly (Oke, Johnson, Steyn, & Watson, 1991). Even more impactfully, high solar (shortwave) radiation loading and consequently elevated temperatures during these times of year mean that pedestrians in cities often experience a high mean radiant temperature (T_{MRT}). T_{MRT} is a summary metric that encompasses all shortwave and longwave radiation absorbed by a pedestrian (Ashrae, 2001). It is becoming increasingly important to reduce excessive T_{MRT} in urban areas, particularly because global climate change and urban development are likely to increase summer air temperature beyond the cooling capabilities of existing heat reduction strategies even when applied with high intensity and in tandem (Krayenhoff, Moustaoui, Broadbent, Gupta, & Georgescu, 2018). Moreover, T_{MRT} is usually the best predictor of the spatial variation of heat exposure and potential heat stress in urban environments during summertime fair weather (Lee, Mayer, & Schindler, 2014; Middel & Krayenhoff, 2019), particularly in hot dry climates. Therefore, reduction of T_{MRT} is typically an effective approach for reducing outdoor heat exposure at the microscale.

Reducing excessive heat in cities can be addressed through urban design strategies that target either the microscale radiation environment (Lai, Liu, Gan, Liu, & Chen, 2019; Oke, 1989), or neighbourhood-scale air temperature (Krayenhoff et al., 2021). Since the ability to offset climate change-induced increases of air temperature is limited (Krayenhoff et. al. 2018), microscale radiative cooling approaches are of increasing importance (Middel & Krayenhoff, 2019). At the microscale, these design strategies often focus on increasing the amount of shade to reduce the radiant load at the street level (Ali-Toudert and Mayer, 2006; Ali-Toudert and Mayer, 2007; Johansson, 2006; Kántor et al., 2016; Kántor et al., 2018; Lindberg & Grimmond, 2011; Shashua-Bar, Pearlmutter, & Erell, 2011; Thorsson, Lindberg, Björklund, Holmer, & Rayner, 2011). This strategy has the benefit of reducing T_{MRT} not only by decreasing the shortwave radiation absorbed by pedestrians, but also by keeping street-level surfaces cooler, so they emit less longwave radiation.

One such urban design strategy that has received much attention in the past few decades is street tree planting (Turner et al., 2022). Trees impact thermal exposure not only by directly shading pedestrians, but also by 1) shading street-level and building surfaces, keeping them cooler and resulting in less longwave radiation emitted towards pedestrians; 2) emitting more longwave radiation toward pedestrians than the cooler sky above; 3) slowing down the wind and altering turbulent heat and moisture transfer; and 4) transpiring, thereby reducing sensible heat flux, cooling the air, and increasing latent heat flux and humidifying the air (Krayenhoff et al., 2020; Picot, 2004; Shashua-Bar et al., 2011). Although the impacts of trees on longwave radiation and wind will tend to increase heat exposure, the reduction of heat exposure caused by shading and transpiration typically dominate during daytime, resulting in a strong cooling effect from trees (Kántor, Kovács, & Takács, 2016; Smithers et al., 2018; Taleghani, Sailor, &

Ban-Weiss, 2016). Tree shade alone provides a strong cooling benefit, and T_{MRT} may be reduced by as much as 20–40 °C (Ali-Toudert & Mayer, 2007; Gulyás, Unger, & Matzarakis, 2006; Kántor, Chen, & Gál, 2018; Middel & Krayenhoff, 2019; Middel, Alkhaled, Schneider, Hagen, & Coseo, 2021).

While trees typically produce daytime cooling effects in city streets, specific configurations of street trees may help optimize reductions of excessive heat, for example, by focusing on street locations most in need of tree shade (Ali-Toudert & Mayer, 2006; Coutts, White, Tapper, Beringer, & Livesley, 2016; Johansson, 2006; Thorsson et al., 2011). Several recent studies help clarify optimal tree shapes and placements to best reduce urban heat and $T_{\mbox{\footnotesize{MRT}}}$ as a function of urban geometry (Gillner, Vogt, Tharang, Dettmann, & Roloff, 2015; Millward, Torchia, Laursen, & Rothman, 2014; Morakinyo, Ouyang, Lau, Ren, & Ng, 2020; Park et al., 2019; Smithers et al., 2018; Zheng, Bedra, Zheng, & Wang, 2018). Although these studies use different metrics, including surface temperature, air temperature, and thermal comfort indices, they generally conclude that clusters of trees with high leaf area indexes (LAIs, or tree canopy density) and high transpiration rates should be planted in broad streets with short buildings to help keep pedestrians cool during hot conditions.

Zheng et al. (2018), Park et al. (2019) and Morakinyo et al. (2020) focused on tree configurations in different street geometries and provided useful guidance regarding optimal tree species choice and configuration for reducing thermal exposure. Zheng et al. (2018) assessed the use of trees to mitigate heat on the north side of an East-West canyon at different building height-to-street width (H/W) ratios and found that denser trees with little space in between them are preferable for cooling pedestrians, especially at low canyon H/W ratios. Park et al. (2019) also assessed trees in an East-West canyon, focusing on tree size and spacing. However, they used a two-dimensional model and therefore did not explicitly represent tree spacing and associated interactions in the along-canyon dimension. Regardless, Park et al. (2019) found that pedestrian $T_{\mbox{\scriptsize MRT}}$ was optimally reduced with either larger trees, or many small trees with little space between them. They also found that the magnitude of T_{MRT} reduction dropped exponentially for small trees, but linearly for large trees, as tree spacing increased. Morakinyo et al. (2020), tested the cooling effect of different tree types (different trunk and tree heights, foliage density, and canopy width) in streets of varying H/W ratios. They found that, although trees in the hottest street canyons (low H/W) should be denser and shorter and wider, the trees planted in narrow and tall canyons should be sparser and taller.

It is important to determine the best use of tree planting resources for heat amelioration, since most municipalities have limited space and funds for tree planting and maintenance. However, only a few studies have attempted to address this issue (Morakinyo et al., 2020; Park et al., 2019; Zheng et al., 2018). In addition, apart from the Park et al. (2019) study with a two-dimensional model, no studies to our knowledge have assessed whether pedestrian T_{MRT} reductions (or cooling more generally) per planted tree changes as a function of existing tree cover. For example, additional tree planting may radiatively cool pedestrians more effectively due to a synergistic effect, similar to that observed for air temperature cooling by urban trees (Ziter, Pedersen, Kucharik, & Turner, 2019), or it may offer consistent (Middel, Chhetri, & Quay, 2015) or diminishing benefits as tree cover increases. The dearth of tools suited to addressing questions related to optimal tree placement probably underlies the lack of study of this topic.

We use a new model of pedestrian thermal exposure, TUF-Pedestrian (Lachapelle et al., 2022), to investigate the effect of sidewalk street tree coverage on pedestrian T_{MRT} . TUF-Pedestrian is a microscale model that captures the radiative impacts of trees and explicitly calculates shortwave and longwave radiation incident on each urban surface (e.g., streets and building walls, separated into sub-facet scale "patches") and on a pedestrian, including multiple reflections of both longwave and

shortwave as well as longwave emission. The energy balance of each sub-facet scale patch is solved for a unique surface temperature at each time step. As a result, the urban surface temperature distribution is represented at high spatial resolution, providing a detailed representation of the longwave radiative environment experienced by a pedestrian over the diurnal period as a function of the presence of trees. The relatively high spatial resolution of TUF-Pedestrian allows for an in-depth analysis of different tree placements and their impacts on pedestrians for a selection of urban geometries. Moreover, TUF-Pedestrian uses a vertically explicit pedestrian consistent with the six directional approach to measuring T_{MRT} , permitting insight into the breakdown of T_{MRT} into its directional radiative components. This attribution of the T_{MRT} signal aids identification of those surfaces that most need to be cooled.

Our overall objective is to understand the relative effectiveness of different coverages of street trees for the reduction of daytime pedestrian radiation exposure during fair weather in a residential area (e.g., Open Lowrise local climate zone with relatively low H/W ratio). Our specific objective is to quantify the relation between sidewalk tree coverage and pedestrian $T_{\rm MRT}$ reduction for different times of day during the summer at midlatitudes, and for different street orientations. In addition, we compare the effects of street trees on longwave versus shortwave contributions to pedestrian $T_{\rm MRT}$.

2. Methodology

To investigate these objectives, we apply the TUF-Pedestrian model to a suite of scenarios. TUF-Pedestrian has been shown to accurately reproduce the impacts of buildings and street trees on pedestrian T_{MRT} (Lachapelle et al., 2022) compared to a unique high resolution dataset acquired with the MaRTy human-biometeorological platform (Middel & Krayenhoff, 2019). Importantly, this model evaluation demonstrated that TUF-Pedestrian is additionally able to capture the directional shortwave and longwave fluxes that compose T_{MRT} across the diurnal cycle with good accuracy.

Here, the 'base case' simulation is representative of an Open Lowrise residential area (Stewart & Oke, 2012) with a relatively tall pedestrian located at one side of the street (Fig. 1f; Supplementary Table 1). All patches in the model domain (which compose the building roofs and walls, and street surfaces) are square and have sides 2 m in length. Building wall and street surface albedos are 0.25 and 0.21, respectively. Pedestrians and varying coverages of street trees are placed between the building and the row of street trees, immediately adjacent to the tree canopy in locations typically occupied by sidewalks (Fig. 1a-e; location B in Supplementary Fig. 1).

Upper boundary conditions for the model simulations were provided by meteorological forcing data measured at the top of a 28 m tower

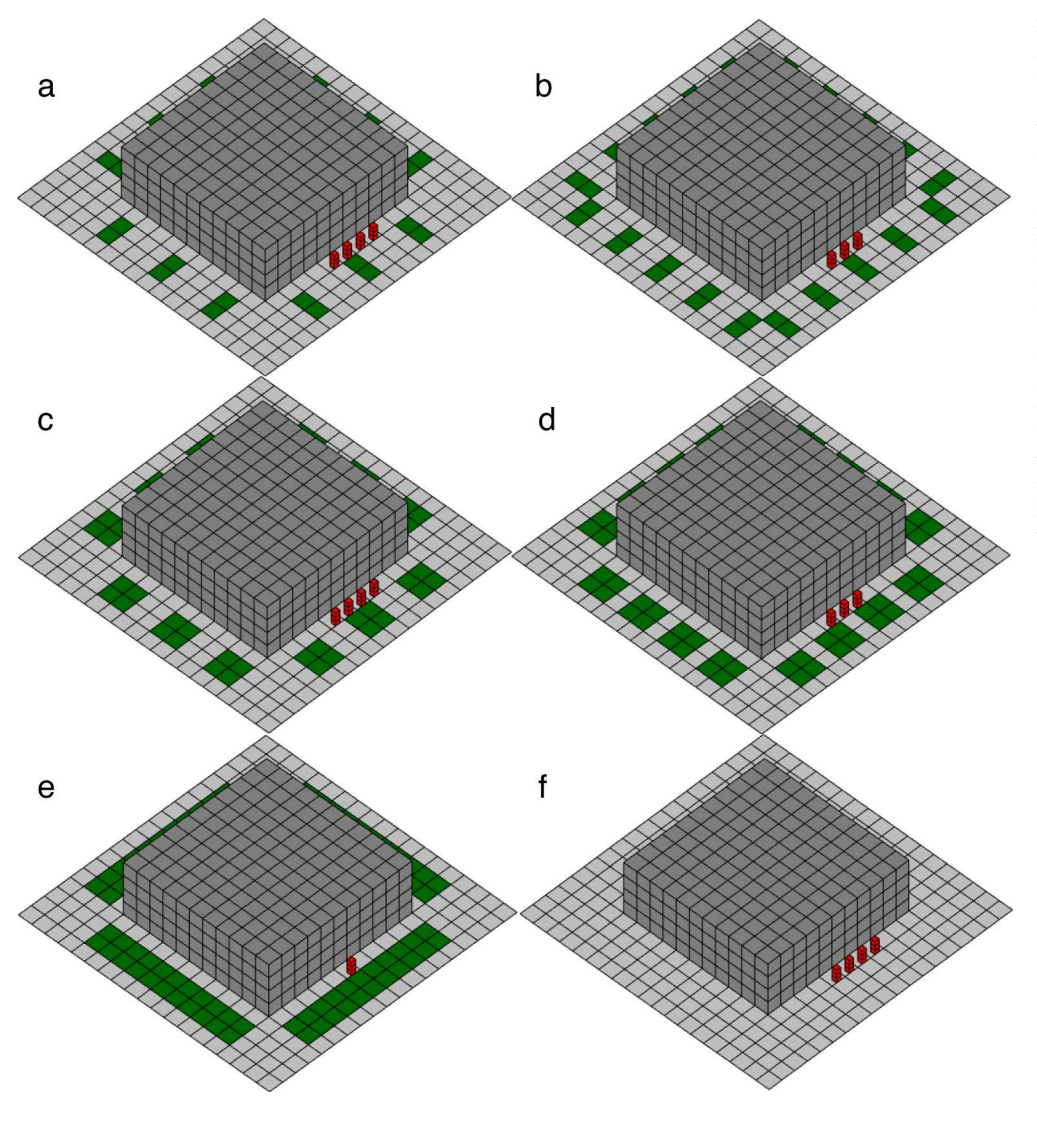


Fig. 1. Excerpts of the simulation domains for simulations with a) 25% sidewalk tree coverage, b) 33% sidewalk tree coverage, c) 50% sidewalk tree coverage, d) 67% sidewalk tree coverage, e) 100% sidewalk tree coverage, and f) 0% sidewalk tree coverage (i.e. base case). Green patches represent the spaces above which the tree foliage is placed, and red sub-patch scale pedestrians show all pedestrian placements required to equally sample the smallest replicable unit of repeated street tree coverage. Here, the "NW" pedestrian location and building orientation are illustrated (assuming North is toward the top of the figure); however, the same relative locations of pedestrians, trees and buildings apply to all other sidewalk pedestrian locations. (For interpretation of the references to colour in this figure legend, the reader is referred to the web version of this article.)

Table 1 Results from linear regressions for each set of simulations in early and late summer during key time periods (peak T_a and peak T_{MRT}), where all p-values < 0.05.

Direction	Season	Time	Intercept (°C)	Slope	R^2	MAD (°C)	RMSD (°C)
N	Early	Ta	-1.03	-12.05	0.96	0.64	0.73
N	Early	T_{MRT}	-0.83	-18.50	0.99	0.49	0.56
N	Late	T_a	-1.79	-18.90	0.96	1.04	1.17
N	Late	T_{MRT}	-0.69	-20.28	0.99	0.41	0.47
NW	Early	T_a	-0.40	-4.41	0.96	0.23	0.28
NW	Early	T_{MRT}	-0.60	-18.28	>0.99	0.35	0.41
NW	Late	T_a	-0.39	-5.61	0.97	0.25	0.29
NW	Late	T_{MRT}	-0.77	-21.66	0.99	0.46	0.52
NE	Early	Ta	-0.70	-17.04	0.99	0.42	0.48
NE	Early	T_{MRT}	-0.54	-17.88	>0.99	0.31	0.37
NE	Late	T_a	-0.53	-17.41	>0.99	0.34	0.39
NE	Late	T_{MRT}	-0.46	-18.82	>0.99	0.27	0.32
E	Early	T_a	-0.46	-15.15	>0.99	0.27	0.31
E	Early	T_{MRT}	-0.80	-16.93	0.99	0.47	0.54
E	Late	Ta	-0.74	-15.50	0.99	0.42	0.48
E	Late	T_{MRT}	-1.58	-21.25	0.98	0.96	1.06
W	Early	T_a	-0.42	-4.43	0.96	0.24	0.28
W	Early	T_{MRT}	-0.72	-19.22	0.99	0.43	0.49
W	Late	T_a	-0.37	-4.01	0.96	0.21	0.25
W	Late	T_{MRT}	-1.13	-21.72	0.99	0.68	0.76
Mean			-0.75	-15.45	0.98	0.45	0.51

located at a latitude of 49.2261° and a longitude of -123.0784° in Vancouver (Christen et al., 2010) during early summer (June 27–28, 2008) and late summer (September 5–7, 2011). For each case, the first day of simulations were considered to be spin-up and were not considered in later analysis. For the late summer simulations, results are a diurnal average of the two subsequent days. Simulations from early summer (~solstice) and late summer (~equinox) at a single location (Vancouver) show the effects of street trees for different diurnal progressions of solar zenith and azimuth angles, and hence yield insight into effects of street tree planting as a function of latitude in addition to day of year (e.g., results from late summer in Vancouver give an indication of how trees impact T_{MRT} differently at higher latitudes close to the solstice).

There are eight different sidewalk locations among streets oriented toward the cardinal directions (N-S and E-W) and additionally rotated 45° relative to cardinal (NE-SW and NW-SE). Simulations were conducted for five of these sidewalk locations, targeting pedestrian locations that are likely to experience high radiative exposure. In the "N" simulations, the pedestrian is placed on the north side of an E-W street canyon. Similarly, in the "NW" simulations, the pedestrian is placed on the north-west side of a NE-SW canyon (45° street orientation), while the pedestrian placement in the "NE" simulations is on the north-east side of a NW-SE street (oriented 45° from N-S and E-W streets). Finally, for a N-S canyon, simulations were performed with the pedestrian on the east side ("E" simulations), and on the west side ("W" simulations) of the canyon. The following locations were excluded because pedestrians are substantively shaded by buildings: the south side of an E-W street, the southwest side of a NW-SE street, and the southeast side of a NE-SW street.

The suite of simulations also includes different sidewalk tree coverages for each pedestrian location: 0 %, 25 %, 33 % 50 %, 67 % and 100 %, corresponding to tree spacings of ∞ , 16 m, 12 m, 8 m, 6 m and 4 m, respectively (Fig. 1). Individual trees are 8 m tall, 4 m wide, with canopy depth of 6 m (trunk height of 2 m), which are the equivalent of a 5-inch caliper tree from the American Nursery Stock Standards. Individual trees for the 25 % and 33 % tree coverage cases are slimmer than the trees in other cases out of necessity given the resolution of the model. The 50 % coverage case was tested with both the normal "square" trees and the slimmer trees found in the 25 % and 33 % coverage cases to ensure the use of slimmer trees yielded consistent results. For each tree coverage, different pedestrian placements are used to sample the smallest replicable unit of tree-covered and uncovered sidewalk (i.e., the combined width of one tree and the gap between it and an adjacent tree; Fig. 1).

These pedestrians are centered on the building face in the along street direction. Results from different pedestrian placements for each tree coverage are averaged together to obtain overall T_{MRT} results for each tree coverage. For the 0 % tree coverage case, four pedestrian placements are used even though only one is needed for the smallest replicable unit, because the four pedestrians allow for provision of an exact base case comparison for each corresponding pedestrian location associated with the different tree coverage simulations.

Results were examined over the diurnal cycle, with a focus on specific times of interest: during peak air temperature (T_a), or peak T_{MRT} . These times of day were determined by examining the times of peak T_{MRT} and peak T_a in the base case simulation without street trees for each of the street orientations. These results indicated peak T_a was 14–18 h in early summer and 14–17 h in late summer, and consistent for all street orientations. Conversely, the daytime period exhibiting peak T_{MRT} was earlier in the day and changed with street orientation and pedestrian location (see Supplementary Fig. 2).

The difference between T_{MRT} averaged over all pedestrian locations for each tree coverage and the average of the corresponding pedestrian locations without trees (0 % coverage) quantifies the effect of tree coverage on pedestrian T_{MRT} . This T_{MRT} difference is then plotted against fractional sidewalk tree coverage for each diurnal period of interest (peak T_{MRT} and peak T_a), and both linear and non-linear regressions are performed to assess the shape of the curve as well as the relative contribution to radiative cooling of street tree planting as a function of existing tree cover (see Sect. 3.1). The form of the equations for the linear and non-linear regressions are as follows:

$$\Delta T_{MRT} = m \times x + b \tag{1}$$

$$\Delta T_{MRT} = c \times \ln(x+1) \tag{2}$$

where \times is the sidewalk street tree coverage fraction, m is the slope, b is the y-intercept, and c is a coefficient. Note that Eq. (2) has a y-intercept of 0 by definition. The performance of these two regressions is compared using the coefficient of determination (\mathbb{R}^2), and by quantifying the bias, mean absolute difference (MAD), and root mean square difference (RMSD), between the regression and the data output by TUF-Pedestrian.

Importantly, TUF-Pedestrian can also determine the relative contributions of different radiative fluxes to the overall radiant cooling effect of trees as expressed by changes to pedestrian T_{MRT} . As such, the difference in radiative fluxes absorbed by the pedestrian from the base case are visualized. The absorbed radiative fluxes are directionally weighted as for the six-directional approach to T_{MRT} calculation (Höppe, 1992),

with lateral fluxes from each cardinal direction being weighted by 0.22 and upward and downward fluxes being weighted by 0.06. This distinction of contributions to T_{MRT} yields insight into which fluxes most strongly control changes in T_{MRT} as a function of tree cover by accounting for the larger area of vertical pedestrian surface (relative to horizontal).

3. Results

3.1. Effect of tree coverage on T_{MRT}

From an urban design standpoint, planners and designers need to know whether or not the addition of trees to shade the sidewalk where

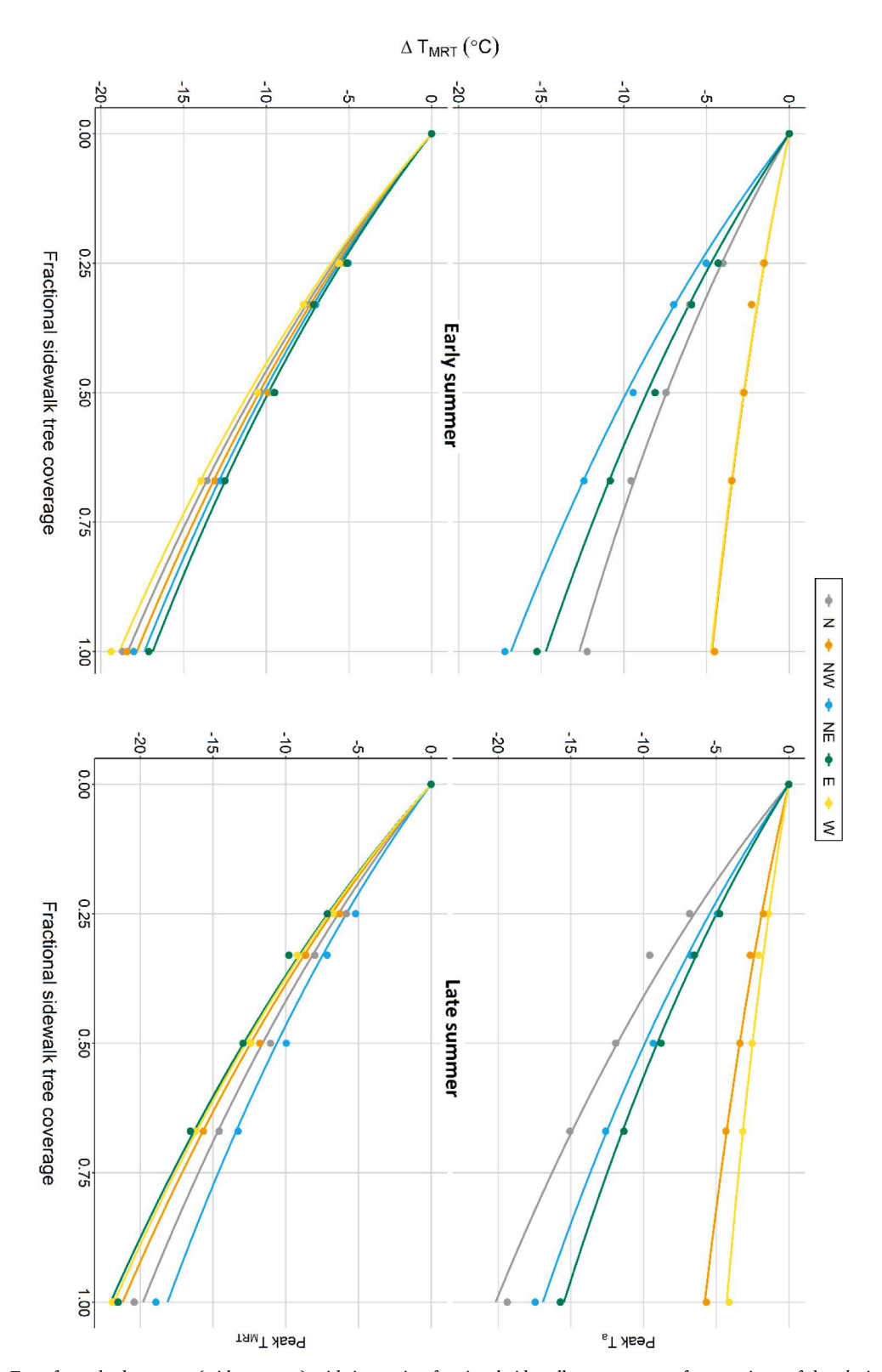


Fig. 2. Difference in T_{MRT} from the base case (without trees) with increasing fractional sidewalk tree coverage for two times of day during two times of year. Logarithmic regressions are shown as the line of best fit.

pedestrians walk provides the same added cooling benefit irrespective of existing tree cover. A range of sidewalk tree cover fractions are tested in terms of their ability to reduce pedestrian T_{MRT}. During the two "hot" afternoon periods of interest (i.e., "peak T_a ", "peak T_{MRT} "), the relationship between sidewalk tree coverage and associated T_{MRT} reduction is approximately linear as indicated by an $R^2 > 0.95$ for all simulations (Table 1). However, the associated best fit equations indicate, based on the y-intercept (i.e., no tree cover), that the case without tree cover results in a -1 °C difference in T_{MRT} (Table 1), when it must be 0 °C by definition. In addition, the residuals from the linear regression shows a clear parabolic pattern, suggesting a non-linear relationship (Supplementary Fig. 3). As such, it is likely that the relationships are slightly non-linear, at least across certain tree coverages. Forcing a logarithmic regression through the origin provides a very good fit, as indicated an R² > 0.99 for all times of day, as well as a lower MAD and RMSD than for the linear regression (Fig. 2, Table 2). Notably, the derivative of this logarithmic fit equation (i.e. Eq. (2)) indicates that planting a tree in a street devoid of trees (x = 0) is about twice as effective at reducing T_{MRT} as planting a tree in a street with nearly full sidewalk street tree coverage $(x \approx 1.0)$:

$$\frac{\partial(\Delta \mathbf{T}_{MRT})}{\partial x} = \frac{c}{x+1} \tag{3}$$

That is, by substituting x=0 and x=1 into Eq. (3), it is apparent that the rate of change of ΔT_{MRT} with added tree density x predicted by this simple mathematical model is twice as large for x=0 compared to x=1.

The relationships in Fig. 2 are only slightly non-linear, and as a result, a linear fit also gives good predictive power with $R^2 > 0.95$ (Table 1). The magnitude of the coefficient in the logarithmic regression (Eq. (2)) and the magnitude of the slope in the linear relationship (Eq. (1)) both provide an estimate of the sensitivity of T_{MRT} to differing tree coverages. These slopes and coefficients during peak T_{MRT} are greater than the corresponding magnitudes for the peak T_a period later in the afternoon. Thus, T_{MRT} shows higher sensitivity to tree coverage during peak T_{MRT} hours, or, in other words, trees are more effective at reducing pedestrian T_{MRT} during peak T_{MRT} hours (peak hours of shortwave radiation loading on the pedestrian).

Across both seasons the pedestrians in the N, NE, and E locations show the highest T_{MRT} sensitivity (i.e., radiative cooling effectiveness) to the sidewalk tree coverages during mid-late afternoon ("peak T_a "), based on the magnitude of slopes for these scenarios (Fig. 2). The NW and W pedestrians show much less T_{MRT} sensitivity at this time. "Peak

 T_a " radiative cooling effectiveness for each pedestrian location, as quantified by the coefficient in the logarithmic fit averaged across both seasons, are: -24.4 (NE), -23.7 (N), -21.8 (E), -7.5 (NW), -6.5 (W) (Table 2). This means that during times of day characterized by high air temperature trees have a greater radiative cooling effect on pedestrians for the NE, N and E pedestrians (in that order of priority), while trees have smaller effect on pedestrian T_{MRT} for the pedestrians located in the NW and W locations, which are shaded by buildings during afternoon hours. A "peak heat" period that is the combination of "peak T_{MRT} " and "peak T_a " periods similarly differentiates the pedestrian locations in terms of tree planting effectiveness (Supplementary Fig. 4). Conversely, all pedestrian locations exhibit similarly high T_{MRT} reductions during midday and early afternoon (i.e., "peak T_{MRT} "; Fig. 2).

3.2. Effects of trees on pedestrian radiative fluxes

Pedestrian T_{MRT} during the day peaks near 70 °C in the absence of street trees but drops below 60 °C when trees are added (Fig. 3). For sidewalks with 100 % tree coverage, maximum T_{MRT} drops to approximately 50 °C or less. The trees assessed here (canopies of 4 m width, 6 m height, and leaf area density 0.5 m^2/m^{-3}) are capable of lowering T_{MRT} by up to approximately 20 °C at particular times of day if trees cover the entire length of the sidewalk (Fig. 4). However, even with 50 % sidewalk coverage, trees can reduce pedestrian T_{MRT} by up to 10-12 °C on average during the middle part of the day. Also notable in Figs. 3 and 4 is that trees are also best at reducing pedestrian T_{MRT} during peak T_{MRT} hours.

TUF-Pedestrian also allows assessment of the directional radiative components contributing to T_{MRT} (Fig. 5 for the N pedestrian, with similar results for other simulations). This makes it possible to examine which fluxes contribute most to pedestrian T_{MRT} and which fluxes the trees modify most strongly in cooling the pedestrian. The lateral longwave fluxes (i.e., those incident on the sides of the pedestrian) are the largest fluxes and contribute most to T_{MRT} (Fig. 5), in agreement with recent observational findings for summertime cases (Middel & Krayenhoff, 2019). However, the increase in T_{MRT} during the day for the base (no tree) case (Fig. 3) is largely attributable to the lateral shortwave fluxes on the sides of the pedestrian facing the sun at a given time of day (Fig. 5). The reflected shortwave radiation and surface temperature distribution across streets and building walls for the 50 % sidewalk tree cover case at 1430 LST for the late summer case illustrates the detailed spatial distribution of the shortwave and longwave radiation environment captured by the TUF-Pedestrian model (Fig. 6). In particular, the shading of the hot south-facing wall by the trees at this time and season

Table 2 Results from logarithmic regressions for each set of simulations in early and late summer during key time periods (peak T_a and peak T_{MRT}), where all p-values < 0.05.

Direction	Season	Time	Intercept (°C)	Coefficient	R^2	Bias (°C)	MAD (°C)	RMSD (°C)
N	Early	Ta	0.00	-18.31	>0.99	-0.08	0.26	0.39
N	Early	T_{MRT}	0.00	-26.51	>0.99	0.06	0.20	0.26
N	Late	T_a	0.00	-29.09	>0.99	-0.18	0.44	0.63
N	Late	T_{MRT}	0.00	-28.58	>0.99	0.12	0.32	0.41
NW	Early	T_a	0.00	-6.75	>0.99	-0.04	0.09	0.16
NW	Early	T_{MRT}	0.00	-25.72	>0.99	0.11	0.31	0.39
NW	Late	T_a	0.00	-8.34	>0.99	-0.02	0.09	0.13
NW	Late	T_{MRT}	0.00	-30.60	>0.99	0.12	0.32	0.42
NE	Early	T_a	0.00	-24.29	>0.99	0.07	0.21	0.27
NE	Early	T_{MRT}	0.00	-25.06	>0.99	0.12	0.34	0.43
NE	Late	T_a	0.00	-24.41	>0.99	0.12	0.32	0.40
NE	Late	T_{MRT}	0.00	-26.15	>0.99	0.15	0.42	0.51
E	Early	T_a	0.00	-21.24	>0.99	0.10	0.28	0.35
E	Early	T_{MRT}	0.00	-24.34	>0.99	0.04	0.19	0.24
E	Late	T_a	0.00	-22.31	>0.99	0.03	0.16	0.19
E	Late	T_{MRT}	0.00	-31.80	>0.99	-0.09	0.26	0.37
W	Early	T_a	0.00	-6.82	>0.99	-0.04	0.10	0.16
W	Early	T_{MRT}	0.00	-27.25	>0.99	0.09	0.26	0.35
W	Late	T_a	0.00	-6.16	>0.99	-0.04	0.09	0.14
W	Late	T_{MRT}	0.00	-31.45	>0.99	0.03	0.18	0.22
Mean			0.00	-22.26	>0.99	0.03	0.24	0.32

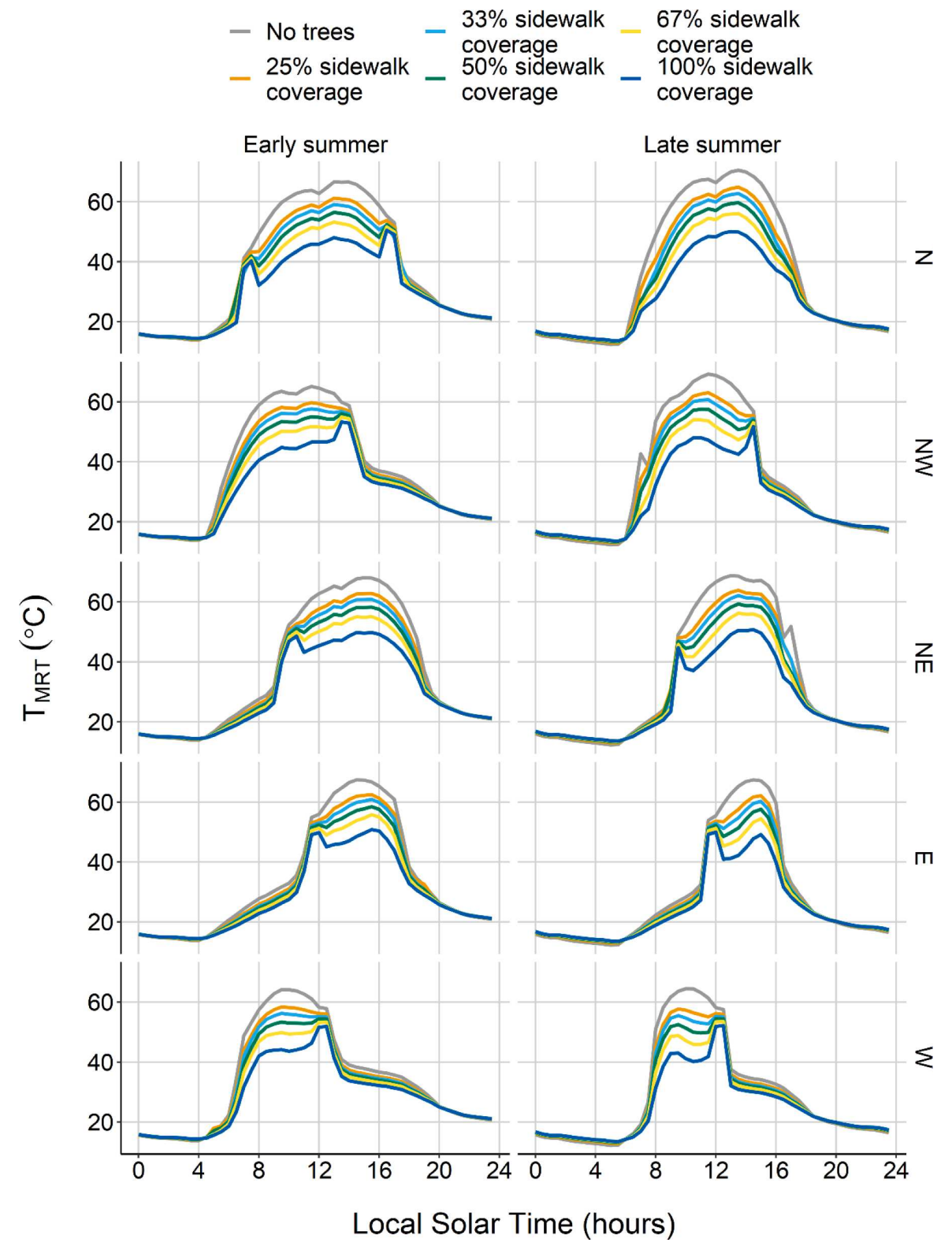


Fig. 3. T_{MRT} over 24 h for early and late summer for different sidewalk tree coverages. Results are shown for each pedestrian location.

(Fig. 6) explains the larger reduction of longwave by trees on the north side of the pedestrian compared to other sides (Fig. 7).

The differences in radiative fluxes incident on the pedestrian as a result of each level of sidewalk tree cover implementation are shown in Figs. 7-11 for the N, NW, NE, E and W pedestrian locations, respectively. Most of the radiative cooling from trees is caused by reduction of shortwave radiation fluxes absorbed by the pedestrian, and in all cases

the decreases in absorbed shortwave radiative fluxes due to tree shading are found predominantly on the sides of the pedestrian facing towards the sun as well as at the top of the pedestrian. Whereas the pedestrian in the N location is affected by direct shortwave radiation for the entire day, the pedestrians in the NW and W location becomes shaded by the building earlier in the afternoon (near 15 h and 12 h respectively), and the pedestrian in the NE and E simulations is shaded by the building



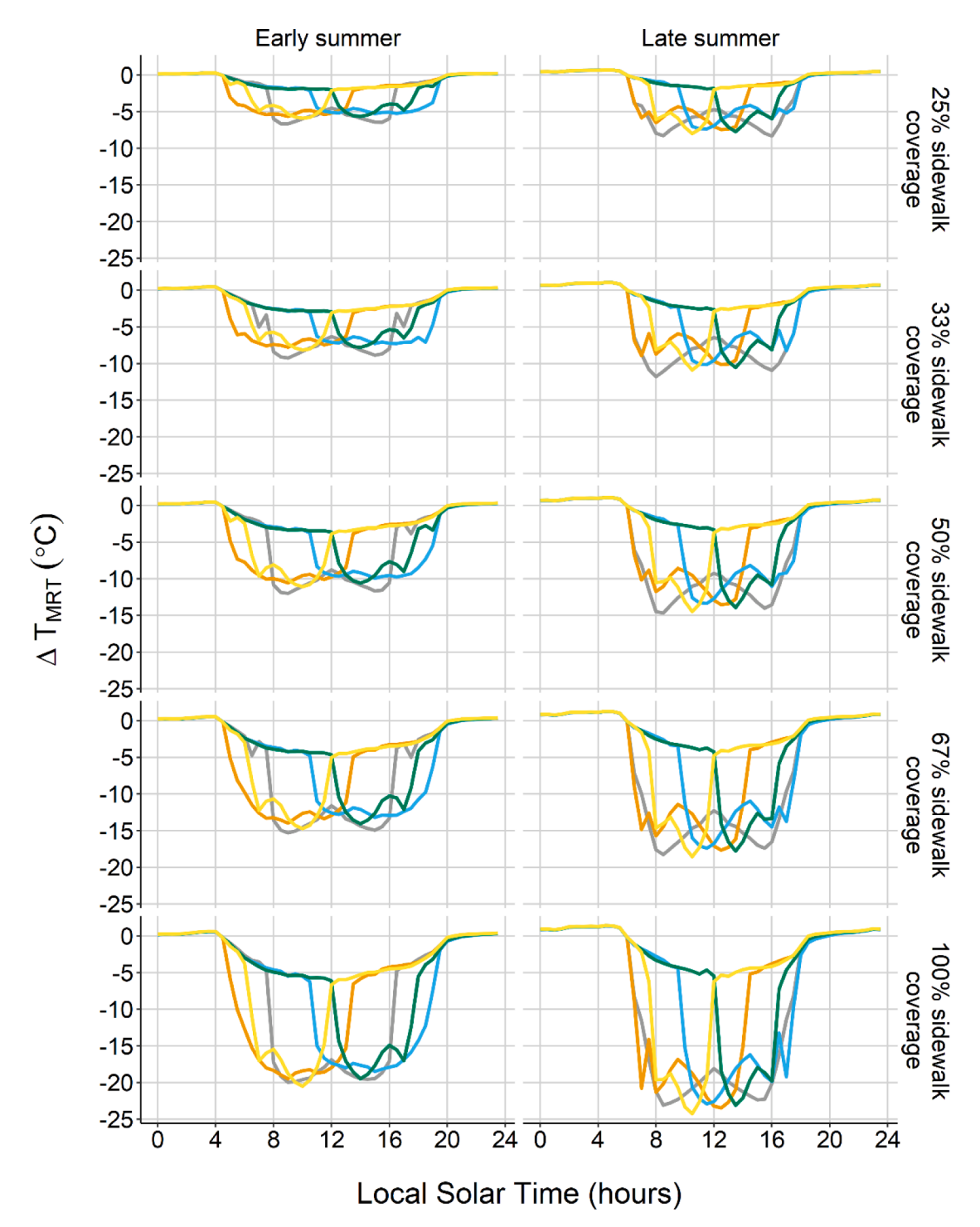


Fig. 4. Difference in T_{MRT} from the case without trees in early and late summer for five different sidewalk tree coverages. Results are shown for the N, NW, NE, E, and W cases.

through most of the morning (until near 10 h and 12 h respectively). The surfaces around the pedestrian are cooled due to the presence of trees (e. g. Fig. 6), which during sunlit periods provides approximately 25 % of the cooling experienced by the pedestrian via reductions in absorbed longwave radiation (Figs. 7-11), increasing to 50 % of cooling during periods of the day when the pedestrian is shaded (Supplementary Fig. 5). During daytime periods when the pedestrian is not in the sun, longwave absorption reductions account for more than half of the total reduction

of radiation absorbed by the pedestrian (Figs. 7-11). Due to the lower sun elevation, trees provide more T_{MRT} reduction over the course of the day for the late summer period compared to the early summer period for the N, NE and NW pedestrian locations. However, the reverse is true for the E and W pedestrian locations because building shade renders tree shade irrelevant for a greater portion of the day during late summer.

Trees decrease longwave fluxes absorbed by the pedestrian throughout the day. For each street orientation, longwave absorption on

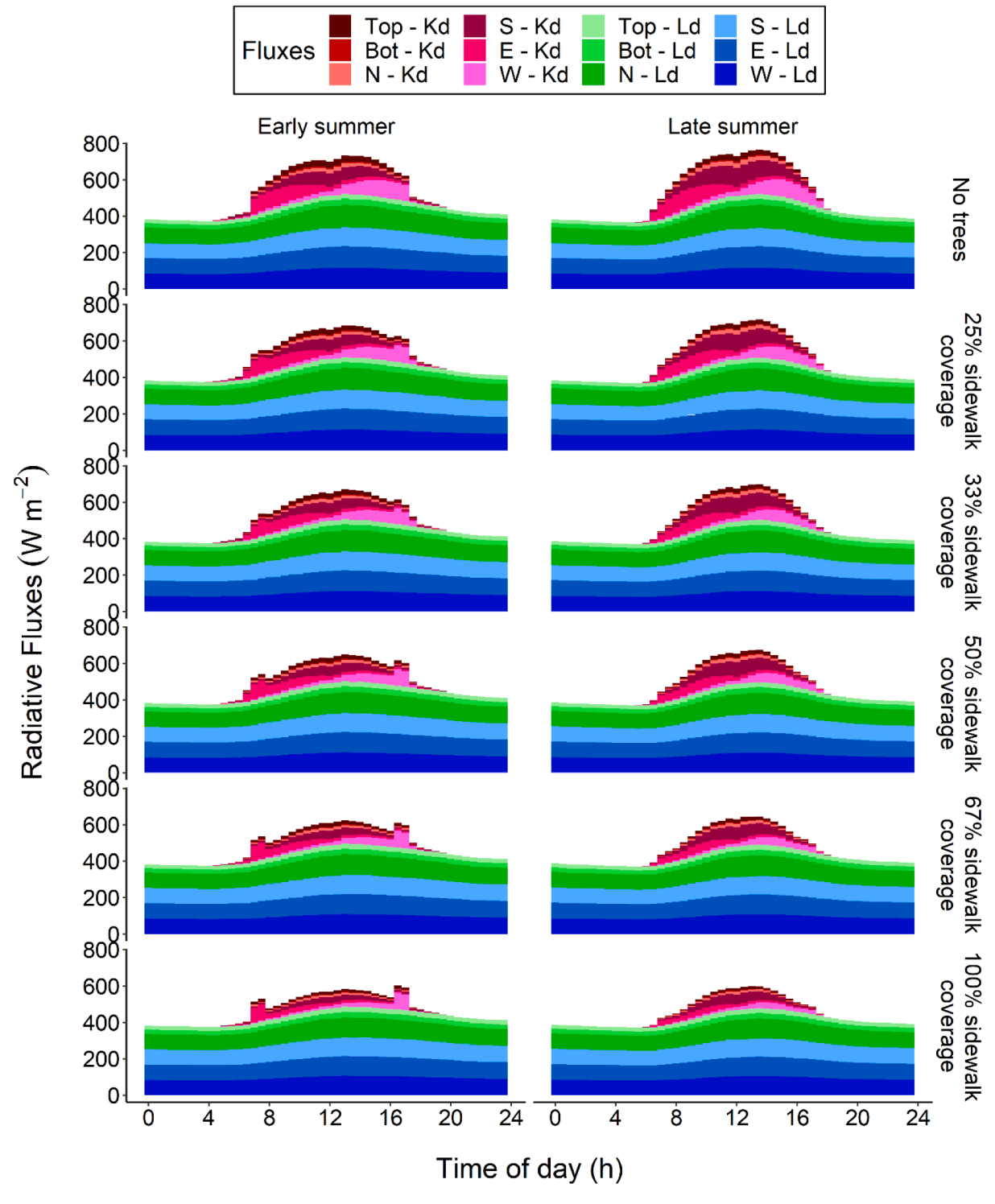


Fig. 5. Weighted radiative fluxes absorbed by the pedestrian for the N pedestrian location (north side of E-W street) for different sidewalk tree coverages and seasons. K_d are shortwave fluxes and Ld are longwave fluxes. Top, Bot, N, S, E, and W represent the six directions: top, bottom, north, south, east, and west, respectively, and the building is directly north of the pedestrian.

the side of the pedestrian facing the building is most affected by the presence of trees, particularly during late summer. The trees provide shade to the otherwise hot building walls facing the pedestrians, which absorb and reflect less shortwave radiation as a result (Fig. 6). The building walls therefore remain cooler (Fig. 6) and emit less longwave radiation towards the pedestrian. Similarly, the ground immediately surrounding the pedestrian is also cooled by tree shade and therefore emits less longwave radiation, decreasing longwave radiative fluxes to

all sides of the pedestrian during the day. At night, longwave radiative fluxes to pedestrians are only slightly affected by trees, in part as a result of two processes that offset each other to different degrees on different sides of the pedestrian. For the pedestrian in the N location (Fig. 7), the north side of the pedestrian receives less longwave radiation at night, while the south side of the pedestrian receives an increased amount, as a result of tree cover. The building has been cooled by tree shade during the day, resulting in less daytime heat storage and release toward the

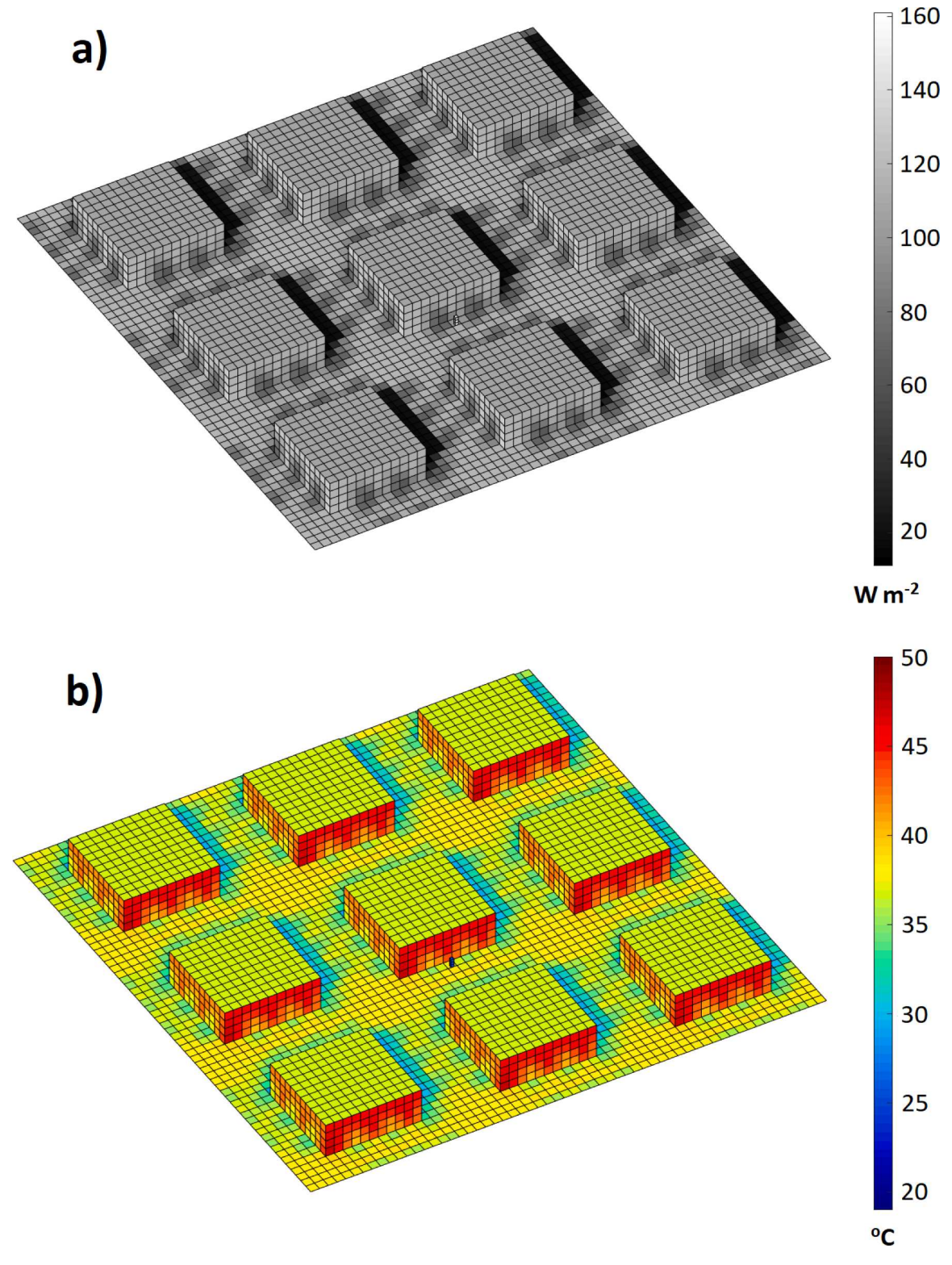


Fig. 6. Reflected shortwave radiation (a) and surface temperature (b) at impervious surfaces at 1430 LST for the late summer simulation with 50% sidewalk street tree coverage (i.e. Fig. 1c). North is toward the upper left, aligned with the street direction.

north side of the pedestrian in the form of longwave emissions at night. In contrast, the south side of the pedestrian, which faces the street and the tree cover, sees less cool sky due to the tree cover, and therefore absorbs more longwave radiation as the trees replace the cold sky as primary longwave emitters from this direction.

4. Discussion

We investigated the effect of street trees on pedestrian T_{MRT} using the TUF-Pedestrian model. Our goal was to assist planners and designers further understand how specific sidewalk tree coverages influence pedestrian T_{MRT} to help optimize the use of street trees for T_{MRT}

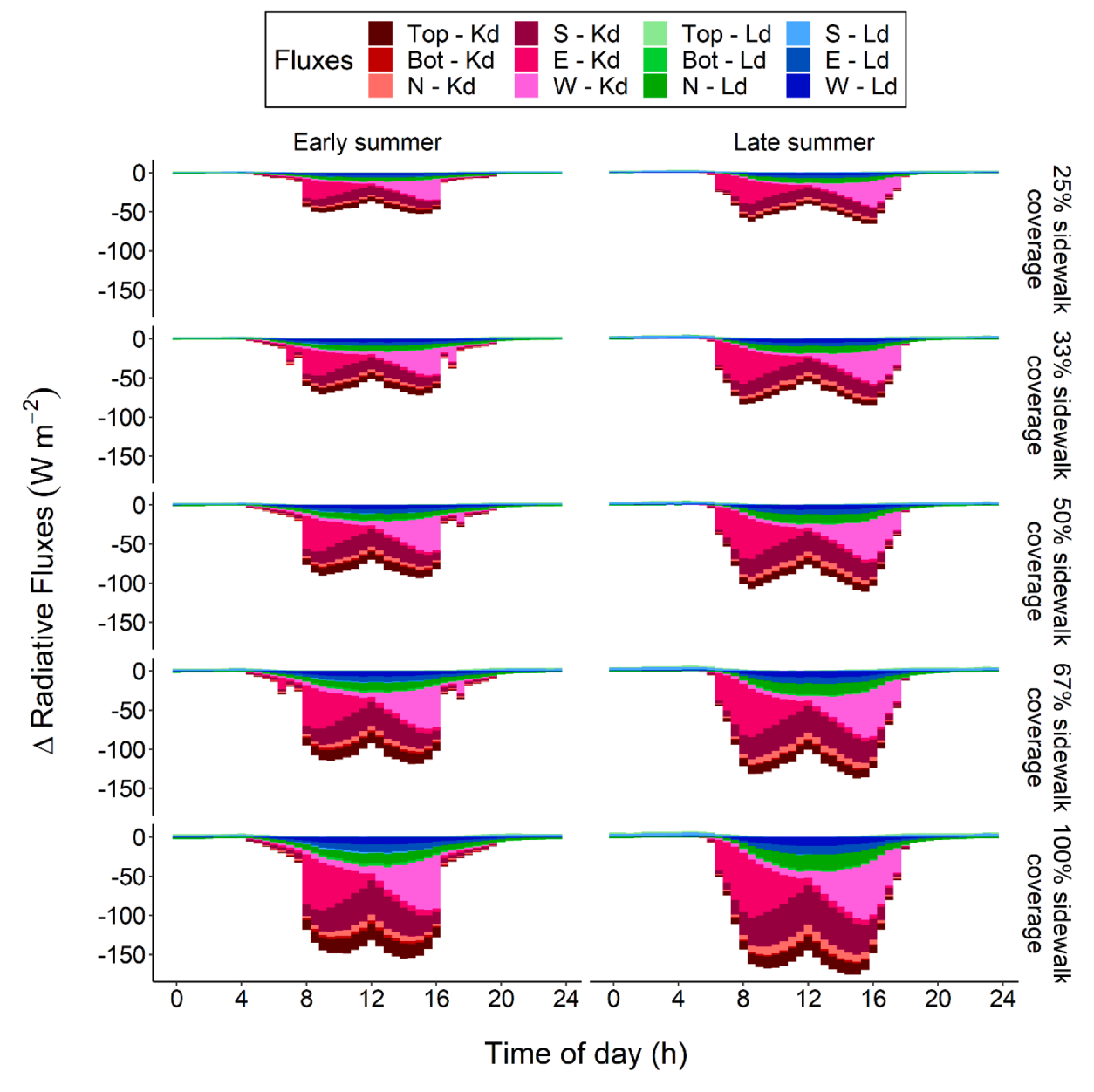


Fig. 7. Difference in weighted radiative fluxes absorbed by the pedestrian from the base case (i.e., no trees) for the N pedestrian location with different sidewalk tree coverages and at two times of year. K_d represents shortwave fluxes and Ld represents longwave fluxes. Top, Bot, N, E, S, and W represent the six directions: top, bottom, north, east, south, and west, respectively, and the building is north of the pedestrian.

reduction, since municipalities often have limited space and funding for planting and maintaining street trees (Salmond et al. 2016). Urban forestry decision-makers need to understand how many trees need to be planted to best cool pedestrians, and to account for limitations and costs associated with street tree planting and maintenance, to optimize their impacts on pedestrian thermal comfort in city streets. Even if plantable space and funding for street trees were not of concern, high tree cover in streets reduces ventilation and has potentially negative consequences for air quality at the pedestrian level (Karttunen, Kurppa, Auvinen, Hellsten, & Järvi, 2020; Norton et al., 2015; Vos, Maiheu, Vankerkom, & Janssen, 2013). Moreover, equity-based justifications for tree planting investments are important. Therefore, there are multiple reasons to better understand the effectiveness of different tree coverages for reducing pedestrian T_{MRT}.

4.1. Radiative cooling effectiveness as a function of sidewalk tree cover

Our simulations indicate that more tree cover is better at radiatively cooling pedestrians in a detached residential area with a low canyon H/W ratio where shade from urban form is sparse. The T_{MRT} reduction effect of trees is a slightly non-linear function of sidewalk tree coverage, and a logarithmic equation indicating monotonically decreasing radiative cooling effectiveness of street trees with increasing total sidewalk tree cover provides a good fit to the available simulation data (Eq. (2), Fig. 2). However, we hypothesize that the diminishing T_{MRT} reduction returns as tree cover increases simulated here results from mutual shading between trees, which is unlikely to play a substantive role for low tree coverages (individual trees are equally spaced in all scenarios we consider here). It is more likely that cooling is relatively linear (i.e., effectiveness per tree is constant) up to a certain sidewalk tree coverage, and thereafter increasingly diminishes as mutual shading plays an

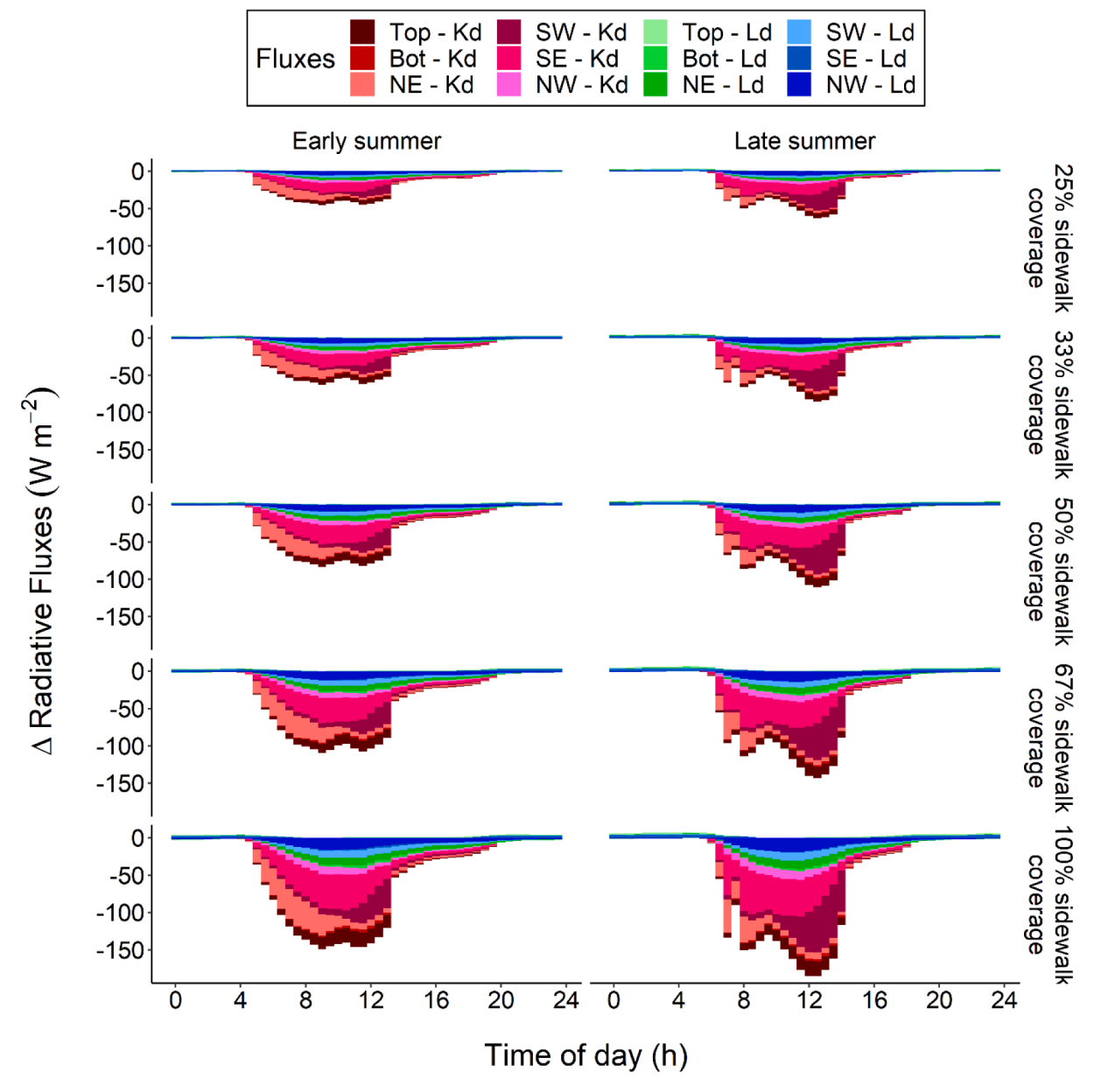


Fig. 8. Same as Fig. 7 except for the NW pedestrian location. Top, Bot, N, E, S, and W represent the six simulated sides of the pedestrian, where N indicates the side facing the building, to the north-west of the pedestrian.

increasing role. Notably, T_{MRT} reduction per tree coverage increase is about 1.5–2 times as large for the increase in tree coverage from 0.00 to 0.25 as it is for the increase in tree coverage from 0.67 to 1.00 (not shown). Similarly, the logarithmic fit (Eq. (2), Fig. 2) indicates a doubling of radiative cooling per street tree for a street without trees compared to a street approaching full sidewalk tree coverage. Regardless, the results presented here clearly indicate that space between individual street trees should be maximized to optimize radiative cooling per tree. Many municipalities space street trees at 8 m (25ft) on center based on decades old prescriptive guidance and tradition (Whyte, 1980). A question for future research for improved pedestrian cooling per street tree is determination of the degree of sidewalk street tree coverage (and the associated tree spacing) at which mutual shading begins to substantially decrease radiative cooling effectiveness as a function of season, latitude, and tree characteristics.

A linear function also captures the dependence of T_{MRT} reduction on sidewalk street tree cover reasonably well. Park et al. (2019) have also addressed the relationship between tree coverage and pedestrian T_{MRT}

reduction. Using a 2-D model that does not explicitly represent tree spacing and associated interactions in the along-canyon direction, they suggest that $T_{\mbox{\footnotesize{MRT}}}$ drops exponentially with increasing tree coverage. Their results for tree sizes that approximate the current work show a different relationship between sidewalk tree coverage and T_{MRT} reduction (Fig. 12). Both our TUF-Pedestrian results and the Park et al. (2019) results show the intuitive result that more trees give more radiative cooling, yet unlike the Park et al. (2019) study, TUF-Pedestrian indicates that effectiveness of tree planting for T_{MRT} reduction decreases much more slowly with increased tree coverage (Fig. 12). The current simulations improve on the work of Park et al. (2019) by explicitly representing tree spacing and associated interactions in the along-canyon dimension by using a 3-D model. Nevertheless, both our study and Park et al. (2019) clearly indicate that a higher percentage of sidewalk tree cover will help further reduce pedestrian T_{MRT} in hot weather, and more study is needed to better quantify these relations. In addition to mutual shading, street tree planting decisions will also need to consider funding, available space, street ventilation, and related factors.

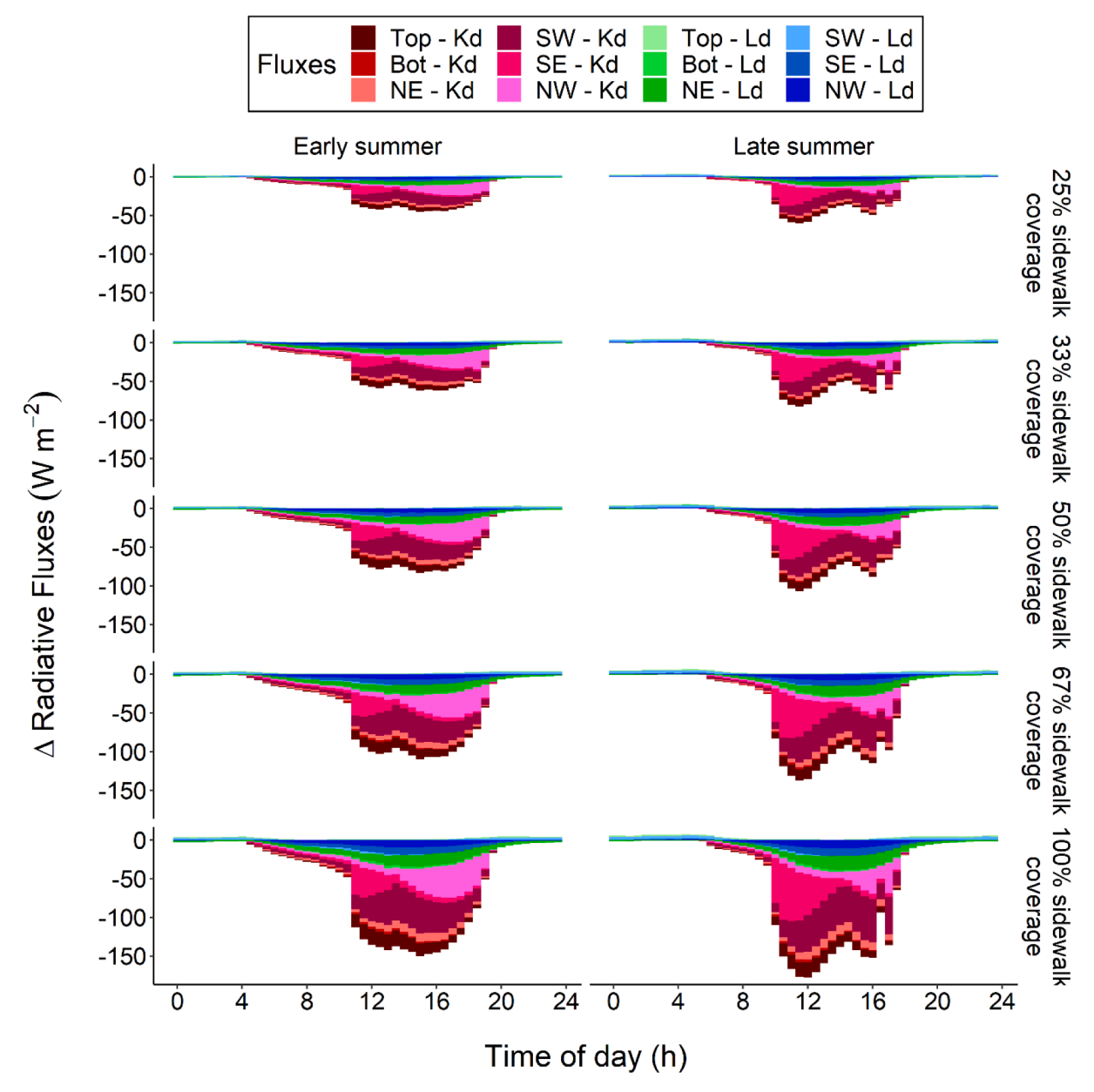


Fig. 9. Same as Fig. 7 except for the NE pedestrian location. Top, Bot, N, E, S, and W represent the six simulated sides of the pedestrian, where N indicates the side facing the building, to the north-east of the pedestrian.

4.2. Radiative cooling effectiveness as a function of street orientation and pedestrian location

The afternoon period when T_{MRT} and/or Ta peak is likely the most important period to provide radiative cooling to pedestrians. However, trees exhibit larger or smaller cooling effects at these times of day depending on the street orientation. Trees have little cooling effect on pedestrians located on the north-west side of a NE-SW canyon during the afternoon period because the proximity of the pedestrian to the building provides ample shade at that time. In contrast, trees will have a greater cooling effect on pedestrians located on the north-side of an E-W canyon, or on pedestrians located on the north-east side of a NW-SE canyon. Pedestrians located on the west side of a N-S canyon are also less effectively cooled by trees due to the building shade in the afternoon. Conversely, trees have a greater cooling effect on a pedestrian on the east side of a N-S canyon in the afternoon. Therefore, *ceteris paribus*, the planting of trees should be focused on locations where trees have a greater effect during the hot afternoon period. These locations would be

those that are most exposed to the sun and have little shade from buildings during summer afternoons: e.g., the north side of an E-W canyon with relatively short buildings. Additionally, neighbourhoods where sidewalks are not directly adjacent to buildings (i.e., there are setbacks) would also benefit from more tree cover to decrease pedestrian T_{MRT}. These findings advance a more nuanced planning and design approach to strategically prioritize the diurnal pedestrian comfort needs for specific sidewalk segments and activities. This more refined approach is helpful for transportation planning related to transit stops and critical pathways used by pedestrians during their daily necessary (e.g., work), optional (e.g., stroll), and social (e.g., walking club) activities (Gehl, 1987).

4.3. Directional radiative fluxes and contributions to T_{MRT}

By quantifying directional shortwave and longwave fluxes incident on pedestrians with TUF-Pedestrian, we can also indicate the surfaces that most strongly modulate T_{MRT} . For the current midlatitude

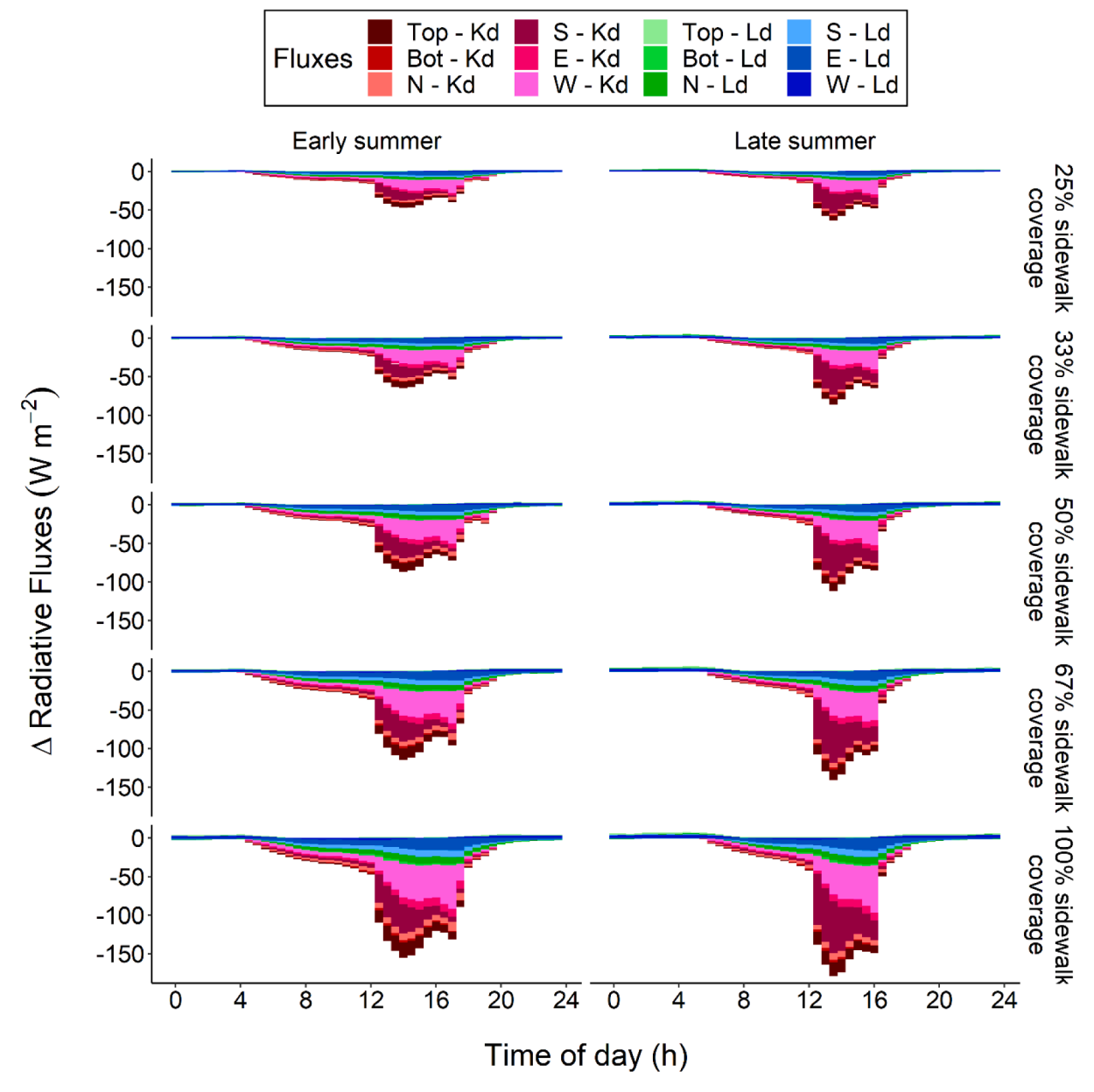


Fig. 10. Same as Fig. 7 except for the E pedestrian location. Top, Bot, N, E, S, and W represent the six simulated sides of the pedestrian, where N indicates the side facing the building, to the east of the pedestrian.

simulations, we find that longwave lateral fluxes dominate pedestrian T_{MRT} (Fig. 5), and that cooling nearby building walls could substantively lower T_{MRT}, in agreement with Middel and Krayenhoff (2019). However, trees primarily reduce T_{MRT} by reducing the shortwave fluxes incident on a pedestrian, particularly the lateral shortwave fluxes (e.g., Fig. 7). TUF-Pedestrian shows a smaller effect on longwave radiative fluxes as a result of tree planting, especially at night (e.g., Figs. 4 and 7). This effect on longwave emissions at night is smaller than the 5 $^{\circ}\text{C}$ increase of T_{MRT} found by Middel and Krayenhoff (2019), which may be due in part to the relatively low leaf area density used in the current TUF-Pedestrian simulations. It may be beneficial to use cooling methods other than trees to lower longwave radiative fluxes on pedestrians during the day, such as altering material radiative and/or thermal properties. A better understanding of vertical surfaces provides much needed guidance to pedestrian level design guidance to improve thermal comfort. However, surface temperatures and resulting longwave radiative fluxes can be difficult to reduce in hot weather. Thus, reducing shortwave fluxes (i.e., shade provision) is likely to be the best method to reduce T_{MRT}.

4.4. Assumptions, limitations, and future work

Our simulations focused on the effects of street tree cover on pedestrian T_{MRT} and its radiative fluxes, and they assumed that pedestrian walkways were situated a certain distance from the buildings and immediately adjacent to the edge of the canopy of street trees (e.g., Fig. 1). To assess the impact of the location of pedestrians relative to trees and buildings (i.e. laterally across the street), we simulated several pedestrian locations for the N, NW and NE cases, that is, locations ranging from directly underneath the center of the row of street trees, to locations in the space between the tree canopy and the building (Supplementary Fig. 1). These simulations reveal that the relationship between the placement of the pedestrian walkway in relation to the row of street trees and the reduction of $T_{\mbox{\footnotesize{MRT}}}$ is complex, where the coolest pedestrian locations at the hottest times of day depend on street orientation and solar angle (Supplementary Fig. 6 and Supplementary Discussion). T_{MRT} differences as a function of cross-street pedestrian location reach ~5 °C, much of which probably results from the shape of

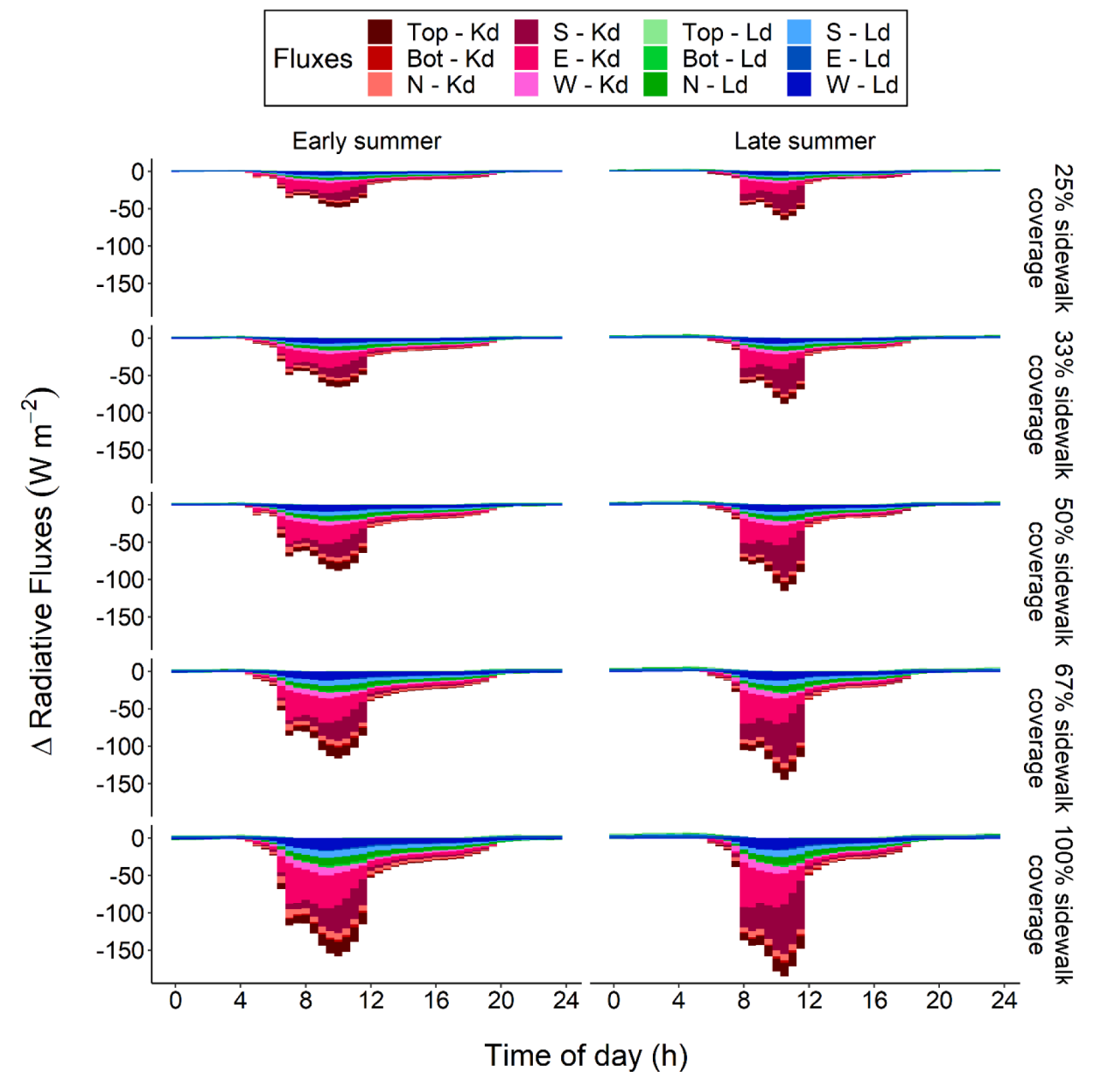


Fig. 11. Same as Fig. 7 except for the W pedestrian location. Top, Bot, N, E, S, and W represent the six simulated sides of the pedestrian, where N indicates the side facing the building, to the west of the pedestrian.

the trees and their position relative to the pedestrian, which controls the degree of attenuation of direct shortwave radiation through the tree canopy. The cross-street pedestrian location at the edge of the tree canopy crowns chosen for the main numerical experiments in this work achieves a relatively high level of T_{MRT} reduction across street directions and seasonal periods tested (i.e., "1.33 m" location in Supplementary Fig. 6).

More study on the relationship between the placement of trees in relation to pedestrians and the reduction in T_{MRT} is still needed. The experiments performed here could be expanded to include simulations with other canyon H/W ratios and different street tree dimensions to increase the range of neighbourhoods captured in the analysis. Addition of overlapping tree crowns could be added in the model (i.e., by increasing the leaf area density in areas of overlap). In addition, results may change for ground and wall surface albedos that differ from those assumed here (0.21 and 0.25, respectively). For example, lower street surface albedo (e.g. 0.10–0.15, more typical of asphalt), would decrease shortwave reflection incident on pedestrians for the 'no tree' case and

therefore slightly reduce effectiveness of street tree planting for T_{MRT} reduction. Finally, the current analyses use specific dimensions and diurnal sequences of solar angles, which may not be generalizable to different canyon or tree dimensions or latitude-season combinations. Ultimately, results from this type of study should be non-dimensionalized to be more widely applicable.

5. Conclusions

The practice of heat management in cities is an emerging 21st century trend, but it's underdeveloped (Hamstead & Coseo, 2019). As our study illustrates, communities of practice could benefit from more sophisticated guidance related to the cooling of pedestrian spaces that goes beyond traditional metrics such as satellite-based surface temperature or air temperature. Stone (2019) challenges planners to think of heat as an invisible, non-episodic, and city-amplified challenge. A key reframe Stone makes is that heat challenges do not necessarily subside with the heat wave. Air temperatures can be within a 'comfortable' range, but

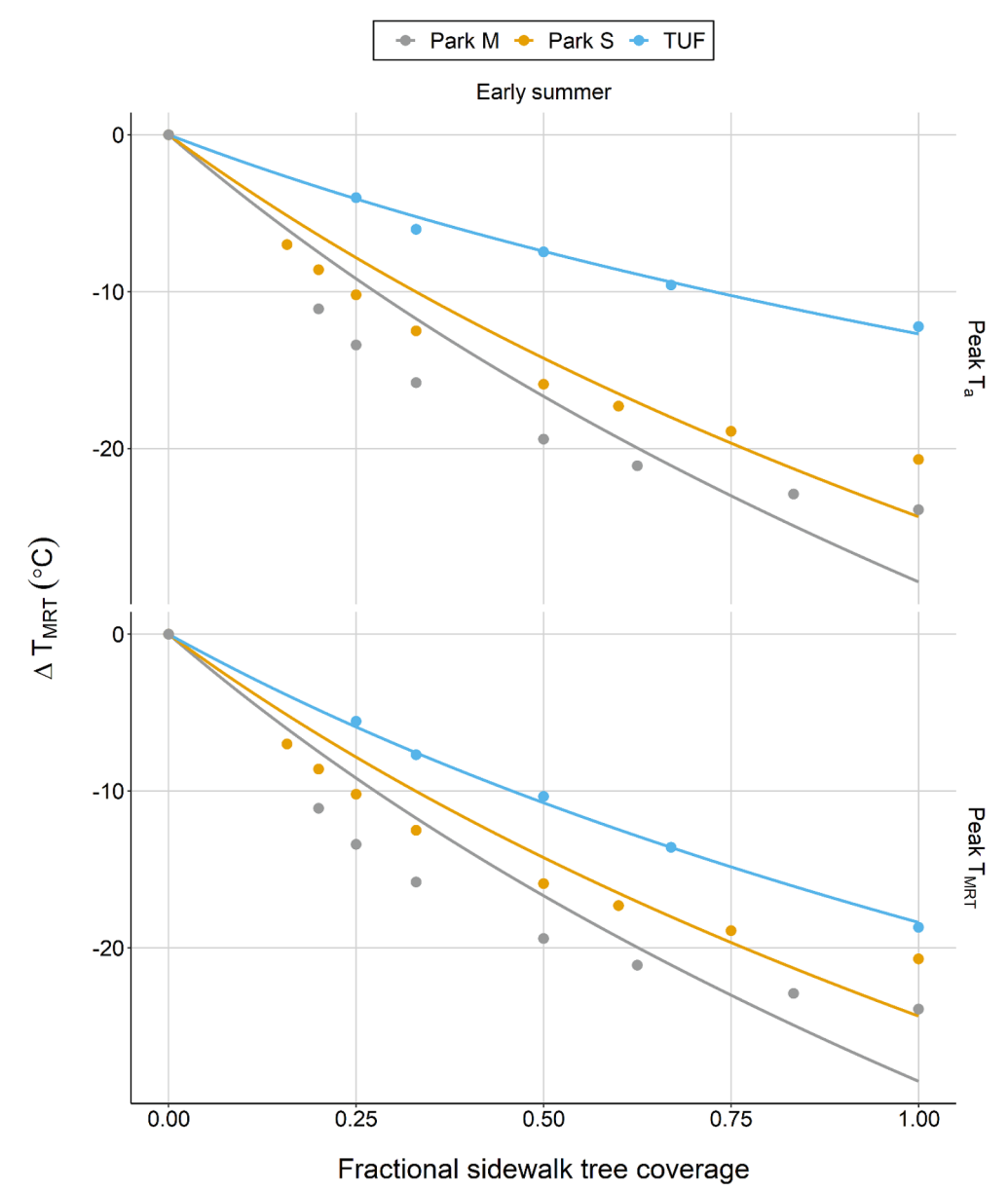


Fig. 12. Reduction of T_{MRT} as a function of increasing fractional sidewalk tree coverage on the north side of an E-W street for the early summer TUF-Pedestrian simulation (trees are 8.0 m tall, 4.0 m wide, LAD = 0.5m²/m⁻³), compared to simulated summertime data from Park et al. (2019) for their "S" $(5.9 \text{ m tall}, 3.0 \text{ m wide}, LAD = 1.0 \text{ m}^2/\text{m}^{-3})$ and "M" (9.5 m tall, 5.0 m wide, LAD = 1.0m²/m⁻³) trees. Attempted logarithmic fits (gray and orange lines) for Park et al. (2019) data are included to demonstrate the different shape of the relation they derive. (For interpretation of the references to colour in this figure legend, the reader is referred to the web version of this article.)

solar radiation loading on pedestrians due to a lack of shade can create excessive heat conditions in city streets in many bioclimatic regions. The approach taken here integrates $T_{\rm MRT}$ to evaluate three-dimensional thermal impacts on sidewalk spaces including wall and pavement materiality, solar orientation and shade patterns, vegetation, and radiational dynamics, emphasizing the importance of radiation to measuring what matters – comfort and health. An approach which integrates $T_{\rm MRT}$ as a key component of the heat experience in cities begins to more holistically capture the thermal-radiative life in which we inhabit. Ultimately, more complete metrics that capture the complete pedestrian experience of heat, such as the Universal Thermal Climate Index (UTCI; Jendritzky, de Dear, & Havenith, 2012), should be used. $T_{\rm MRT}$ is a key component of UTCI, and typically controls most of its spatial variation in urban areas during hot conditions.

Here, the TUF-Pedestrian energy balance, radiation and thermal exposure model is applied to quantify the effectiveness of sidewalk street tree radiative cooling. Recent model evaluation demonstrates that TUF-Pedestrian accurately captures both shortwave and longwave directional radiation fluxes absorbed by pedestrians and the resulting mean radiant temperature (T_{MRT}) for pedestrian locations that are both

adjacent to and directly underneath urban tree cover (Lachapelle et al., 2022). Simulations presented here demonstrate that optimal implementation of street trees to reduce pedestrian T_{MRT} can be complex and depend on several factors. The specific focus here is the placement of different coverages of evenly-spaced trees along the sidewalk and associated radiative impacts on pedestrians. A key result of the current simulations is that while more sidewalk street trees provide greater T_{MRT} reduction, once a certain level of tree cover is reached they do so with modest reductions of radiative cooling effectiveness per tree. Analysis of the current simulation results indicates that tree planting on a street with ≈100 % existing sidewalk street tree coverage is approximately 50-70 % as effective as planting on a street without trees. We hypothesize that reductions of radiative cooling effectiveness result from mutual shading between individual trees, which is not expected to play a substantive role until a certain sidewalk street tree coverage is reached; provided this hypothesis is accurate, the T_{MRT} reduction per tree is expected to remain approximately constant below this tree coverage and decrease for higher tree coverages.

A second key result is that specific pedestrian locations in specific street orientations (i.e., north side of east-west street, east side of north-

south street, and northeast side of northwest-southeast street) exhibit larger T_{MRT} reductions during the hottest periods of the day as a result of tree planting. Alongside recent evidence that trees reduce air temperature more effectively as tree canopy coverage increases (Ziter et al., 2019), the current results suggest that, while more trees provide both more air temperature and T_{MRT} reductions, a relatively evenly-spaced distribution of sidewalk street trees across all sun-exposed street locations in a block or neighbourhood may be optimal from the perspective of reducing outdoor heat exposure during warm conditions (i.e., it would maximize both air temperature cooling and radiative cooling). Additional considerations may alter this conclusion for any particular neighbourhood, such as air quality considerations, or the number of pedestrians frequenting any particular street, and their relative vulnerability to heat.

Simulation results indicate that trees affect T_{MRT} during daytime primarily by reducing shortwave radiative fluxes incident on pedestrians. Trees also cool surrounding street and building wall surfaces, reducing longwave fluxes towards pedestrians. Notably, reduction of longwave emission from surfaces shaded by trees contributes approximately 25 % of the total reduction of radiation absorbed by the pedestrian when the pedestrian would otherwise be exposed to full sunlight. For the midlatitude summer conditions studied here, longwave radiative fluxes make up the majority of the daytime radiation (and 100 % of nighttime radiation) absorbed by the pedestrian as encapsulated by the T_{MRT} metric. However, contributions of absorbed shortwave radiation to T_{MRT} are most readily altered by tree planting (or building shade). Nevertheless, implementation of design strategies other than trees that reduce longwave emissions (such as changing surface materials) may additionally help reduce pedestrian T_{MRT} during hot periods. We suggest further study into the specific implementation of street trees in different urban geometries, latitudes and seasons to best understand how to maximize the cooling effects of trees on pedestrians.

Declaration of Competing Interest

The authors declare that they have no known competing financial interests or personal relationships that could have appeared to influence the work reported in this paper.

Data availability

Data will be made available on request.

Acknowledgements

Thanks are due to Claudia Wagner-Riddle for providing comments on an early version of this manuscript. Funding was provided by an NSERC Discovery Grant to ESK.

Appendix A. Supplementary data

Supplementary data to this article can be found online at https://doi.org/10.1016/j.landurbplan.2022.104608.

References

- Ali-Toudert, F., & Mayer, H. (2006). Numerical study on the effects of aspect ratio and orientation of an urban street canyon on outdoor thermal comfort in hot and dry climate. *Building and Environment*, 41, 94–108. https://doi.org/10.1016/j. buildenv.2005.01.013
- Ali-Toudert, F., & Mayer, H. (2007). Effects of asymmetry, galleries, overhanging façades and vegetation on thermal comfort in urban street canyons. Solar Energy, 81, 742–754. https://doi.org/10.1016/j.solener.2006.10.007
- Ashrae. (2001). ASHRAE Fundamentals Handbook 2001 ((SI Edition)). American Society of Heating, Refrigerating, and Air- Conditioning Engineers.
- Christen, A., Coops, N., Kellett, R., Crawford, B., Heyman, E., Olchovski, I., ... van der Laan, M. (2010). A LiDAR-based urban metabolism approach to neighbourhood scale energy and carbon emissions modelling. University of British Columbia supported by Natural Resources Canada.

- Coutts, A. M., White, E. C., Tapper, N. J., Beringer, J., & Livesley, S. J. (2016). Temperature and human thermal comfort effects of street trees across three contrasting street canyon environments. *Theoretical and Applied Climatology*, 124, 55–68. https://doi.org/10.1007/s00704-015-1409-y
- Dosio, A., Mentaschi, L., Fischer, E. M., & Wyser, K. (2018). Extreme heat waves under 1.5 C and 2 C global warming. *Environmental Research Letters*, 13(5), Article 054006. Duneier, M. (2001). Sidewalk. Macmillan.
- Dzyuban, Y., Hondula, D. M., Vanos, J. K., Middel, A., Coseo, P. J., Kuras, E. R., & Redman, C. L. (2022). Evidence of alliesthesia during a neighborhood thermal walk in a hot and dry city. *Science of the Total Environment, 834*, Article 155294.
- Forsyth, A. (2015). What is a walkable place? The walkability debate in urban design. Urban design international, 20(4), 274–292.
- Gehl, J. (1987). Life between buildings (Vol. 23). New York: Van Nostrand Reinhold.
- Gillner, S., Vogt, J., Tharang, A., Dettmann, S., & Roloff, A. (2015). Role of street trees in mitigating effects of heat and drought at highly sealed urban sites. *Landscape and Urban Planning*, 143, 33–42. https://doi.org/10.1016/j.landurbplan.2015.06.005
- Gulyás, Á., Unger, J., & Matzarakis, A. (2006). Assessment of the microclimatic and human comfort conditions in a complex urban environment: Modelling and measurements. Building and Environment, 41(12), 1713–1722. https://doi.org/ 10.1016/j.buildenv.2005.07.001
- Hamstead, Z., & Coseo, P. (2019). Critical Heat Studies: Making Meaning of Heat for Management in the 21st Century—Special Issue of the Journal of Extreme Events Dedicated to Heat-as-Hazard. *Journal of Extreme Events*, 6(03n04), 2003001.
- Höppe, P. (1992). A new procedure to determine the mean radiant temperature outdoors. Wetter Und Leben, 44, 147–151.
- Jacobs, J. (1961). The Death and Life of Great American Cities. Random House.
 Jendritzky, G., de Dear, R., & Havenith, G. (2012). UTCI—why another thermal index?
 International journal of biometeorology, 56(3), 421–428.
- Johansson, E. (2006). Influence of urban geometry on outdoor thermal comfort in a hot dry climate: A study in Fez, Morocco. Building and Environment, 41, 1326–1338. https://doi.org/10.1016/j.buildenv.2005.05.022
- Kántor, N., Chen, L., & Gál, C. V. (2018). Human-biometeorological significance of shading in urban public spaces—Summertime measurements in Pécs, Hungary. Landscape and Urban Planning, 170, 241–255. https://doi.org/10.1016/j. landurbplan.2017.09.030
- Kántor, N., Kovács, A., & Takács, Á. (2016). Small-scale human-biometeorological impacts of shading by a large tree. Open Geosciences, 8, 231–245. https://doi.org/ 10.1515/geo-2016-0021
- Karttunen, S., Kurppa, M., Auvinen, M., Hellsten, A., & Järvi, L. (2020). Large-eddy simulation of the optimal street-tree layout for pedestrian-level aerosol particle concentrations A case study from a city-boulevard. Atmospheric Environment, X, 6 (December 2019), Article 100073. https://doi.org/10.1016/j.aeaoa.2020.100073
- Krayenhoff, E. S., Broadbent, A. M., Zhao, L., Georgescu, M., Middel, A., Voogt, J. A., ... Erell, E. (2021). Cooling hot cities: A systematic and critical review of the numerical modelling literature. *Environmental Research Letters*, 16(5). https://doi.org/10.1088/ 1748-9326/abdcf1
- Krayenhoff, E. S., Jiang, T., Christen, A., Martilli, A., Oke, T. R., Bailey, B. N., ...
 Crawford, B. R. (2020). A multi-layer urban canopy meteorological model with trees
 (BEP-Tree): Street tree impacts on pedestrian-level climate. *Urban Climate*, 32(July
 2019). Article 100590. https://doi.org/10.1016/j.uclim.2020.100590
- Krayenhoff, E. S., Moustaoui, M., Broadbent, A. M., Gupta, V., & Georgescu, M. (2018). Diurnal interaction between urban expansion, climate change and adaptation in US cities. *Nature Climate Change*, 8(12), 1097–1103. https://doi.org/10.1038/s41558-018-0320-9
- Lachapelle, J. A., Krayenhoff, E. S., Middel, A., Meltzer, S., Broadbent, A. M., & Georgescu, M. (2022). A microscale three-dimensional model of urban outdoor thermal exposure (TUF-Pedestrian). *International Journal of Biometeorology*, 66(4), 833–848. https://doi.org/10.1007/s00484-022-02241-1
- Lai, D., Liu, W., Gan, T., Liu, K., & Chen, Q. (2019). A review of mitigating strategies to improve the thermal environment and thermal comfort in urban outdoor spaces. *Science of the Total Environment*, 661, 337–353. https://doi.org/10.1016/j. scitotenv.2019.01.062
- Lee, H., Mayer, H., & Schindler, D. (2014). Importance of 3-D radiant flux densities for outdoor human thermal comfort on clear-sky summer days in Freiburg. Southwest Germany. Meteorologische Zeitschrift, 23(3), 315–330. https://doi.org/10.1127/0941-2948/2014/0536
- Lindberg, F., & Grimmond, C. S. B. (2011). The influence of vegetation and building morphology on shadow patterns and mean radiant temperatures in urban areas: Model development and evaluation. *Theoretical and Applied Climatology*, 105, 311–323. https://doi.org/10.1007/s00704-010-0382-8
- McGreevy, M., Musolino, C., Udell, T., & Baum, F. (2021). The Feasibility of Transitioning Low-density Suburbs into Healthy Walkable Neighbourhoods: The Case of Adelaide. *South Australia. Urban Policy and Research*, *39*(4), 377–396.
- Middel, A., Alkhaled, S., Schneider, F. A., Hagen, B., & Coseo, P. (2021). 50 Grades of Shade. E1820 Bulletin of the American Meteorological Society., 102(9), E1805. https://doi.org/10.1175/bams-d-20-0193.1.
- Middel, A., Chhetri, N., & Quay, R. (2015). Urban forestry and cool roofs: Assessment of heat mitigation strategies in Phoenix residential neighborhoods. *Urban Forestry and Urban Greening*, 14(1), 178–186. https://doi.org/10.1016/j.ufug.2014.09.010
- Middel, A., & Krayenhoff, E. S. (2019). Micrometeorological determinants of pedestrian thermal exposure during record-breaking heat in Tempe, Arizona: Introducing the MaRTy observational platform. Science of the Total Environment, 687, 137–151. https://doi.org/10.1016/j.scitotenv.2019.06.085
- Millward, A. A., Torchia, M., Laursen, A. E., & Rothman, L. D. (2014). Vegetation placement for summer built surface temperature moderation in an urban

- microclimate. Environmental Management, 53(6), 1043–1057. https://doi.org/10.1007/s00267-014-0260-8
- Morakinyo, T. E., Ouyang, W., Lau, K. K. L., Ren, C., & Ng, E. (2020). Right tree, right place (urban canyon): Tree species selection approach for optimum urban heat mitigation – Development and evaluation. *Science of the Total Environment, 719*, Article 137461. https://doi.org/10.1016/j.scitotenv.2020.137461
- Norton, B. A., Coutts, A. M., Livesley, S. J., Harris, R. J., Hunter, A. M., & Williams, N. S. G. (2015). Planning for cooler cities: A framework to prioritise green infrastructure to mitigate high temperatures in urban landscapes. *Landscape and Urban Planning*, 134, 127–138. https://doi.org/10.1016/j.landurbplan.2014.10.018
- Oke, T. R. (1989). The micrometeorology of the urban forest. *Philosophical Transactions Royal Society of London, B, 324*(1223), 335–349. https://doi.org/10.1098/rsth.1089.0051
- Oke, T. R., Johnson, G. T., Steyn, D. G., & Watson, I. D. (1991). Simulation of surface urban heat islands under "ideal" conditions at night Part 2: Diagnosis of causation. Boundary-Layer Meteorology, 56, 339–358. https://doi.org/10.1007/BF00119211
- Oke, T. R., Mills, G., Christen, A., & Voogt, J. A. (2017). *Urban climates*. Cambridge: Cambridge University Press.
- Park, C. Y., Lee, D. K., Krayenhoff, E. S., Heo, H. K., Hyun, J. H., Oh, K., & Park, T. Y. (2019). Variations in pedestrian mean radiant temperature based on the spacing and size of street trees. Sustainable Cities and Society, 48(March), 1–9. https://doi.org/ 10.1016/j.scs.2019.101521
- Picot, X. (2004). Thermal comfort in urban spaces: Impact of vegetation growth. Case study: Piazza della Scienza, Milan. Italy. Energy and Buildings, 36, 329–334. https://doi.org/10.1016/j.enbuild.2004.01.044
- Shashua-Bar, L., Pearlmutter, D., & Erell, E. (2011). The influence of trees and grass on outdoor thermal comfort in a hot-arid environment. *International Journal of Climatology*, 31, 1498–1506. https://doi.org/10.1002/joc.2177
- Smithers, R. J., Doick, K. J., Burton, A., Sibille, R., Steinbach, D., Harris, R., ... Blicharska, M. (2018). Comparing the relative abilities of tree species to cool the

- urban environment. *Urban Ecosystems*, 21(5), 851–862. https://doi.org/10.1007/s11252-018-0761-y
- Stewart, I. D., & Oke, T. R. (2012). Local climate zones for urban temperature studies. Bulletin of the American Meteorological Society, 93(12), 1879–1900. https://doi.org/ 10.1175/BAMS-D-11-00019.1
- Stone, B., Jr (2019). Policy Nook: Heat Waves as Hurricanes: A Comment. Journal of Extreme Events, 6(03n04), 2071001.
- Taleghani, M., Sailor, D., & Ban-Weiss, G. A. (2016). Micrometeorological simulations to predict the impacts of heat mitigation strategies on pedestrian thermal comfort in a Los Angeles neighborhood. Environmental Research Letters, 11(2), Article 024003. https://doi.org/10.1088/1748-9326/11/2/024003
- Thorsson, S., Lindberg, F., Björklund, J., Holmer, B., & Rayner, D. (2011). Potential changes in outdoor thermal comfort conditions in Gothenburg, Sweden due to climate change: The influence of urban geometry. *International Journal of Climatology*, 31(2), 324–335. https://doi.org/10.1002/joc.2231
- Turner, V. K., French, E. M., Dialesandro, J., Middel, A., Hondula, D. M., Ban-Weiss, G., & Abdellati, H. (2022). How are cities planning for heat? Analysis of United States municipal plans. Environmental Research Letters, 17, Article 064054.
- Vos, P. E. J., Maiheu, B., Vankerkom, J., & Janssen, S. (2013). Improving local air quality in cities: To tree or not to tree? *Environmental Pollution*, 183, 113–122. https://doi. org/10.1016/j.envpol.2012.10.021
- Whyte, W. H. (1980). The social life of small urban spaces.
- Zheng, B., Bedra, K. B., Zheng, J., & Wang, G. (2018). Combination of tree configuration with street configuration for thermal comfort optimization under extreme summer conditions in the urban center of Shantou City. *China. Sustainability*, 10(11), 4192. https://doi.org/10.3390/su10114192
- Ziter, C. D., Pedersen, E. J., Kucharik, C. J., & Turner, M. G. (2019). Scale-dependent interactions between tree canopy cover and impervious surfaces reduce daytime urban heat during summer. *Proceedings of the National Academy of Sciences*, 116(15), 7575–7580. https://doi.org/10.1073/pnas.1817561116